UCGE Reports
Number 20056

Department of Geomatics Engineering

Calibration and Analysis of Loran-C Using a Mobile GPS System

(URL: http://www.geomatics.ucalgary.ca/links/GradTheses.html)

by

Bryan R. Townsend

December 1993

THE UNIVERSITY OF CALGARY

CALIBRATION AND ANALYSIS OF LORAN-C USING A MOBILE GPS SYSTEM

BY

BRYAN R. TOWNSEND

A THESIS

SUBMITTED TO THE FACULTY OF GRADUATE STUDIES
IN PARTIAL FULFILMENT OF THE REQUIREMENTS FOR THE
DEGREE OF MASTER OF SCIENCE IN ENGINEERING

DEPARTMENT OF GEOMATICS ENGINEERING

CALGARY, ALBERTA

DECEMBER 1993

ABSTRACT

Recently, two powerful navigation systems have become available for vehicular navigation on a continent wide basis in Canada, namely, the land-based LORAN-C system, and the satellite-based Global Positioning System (GPS).

Initially designed and used as a marine positioning system, LORAN-C's use on land is relatively new and its overall performance is not well known. The factors affecting the propagation of the LORAN-C low frequency (LF) signals over land are outlined and related to LORAN-C accuracy and signal quality. The LORCAL^2 (**LOR**an **CAL**ibration at The University of **CAL**gary), a vehicle-mounted, GPS-based system designed for collecting and analysing LORAN-C and GPS data in kinematic mode is presented along with four case studies of actual surveys.

Results and conclusions from the case studies are presented along with some recommendations. These tests show that the LORCAL^2 system performed satisfactorily and is an effective tool for LORAN-C and GPS signal analysis.

ACKNOWLEDGEMENTS

I wish to acknowledge and thank the individuals and groups who contributed to my graduate work. Without their support, this thesis would have not have been possible for me.

First and foremost, I would like to thank and express my sincere appreciation to my graduate studies supervisor, Professor Gérard Lachapelle for his continuous support and encouragement throughout the course of my graduate studies.

I would also like to thank the many professors, students, and staff in the Department of Geomatics Engineering who have made my time here fruitful and enjoyable. A special acknowledgement and thanks goes to Professor M. Elizabeth Cannon who thought up the acronym LORCAL^2.

Parts of my studies were finacially supported through contracts from the Communications Research Centre, Communications Canada, the Canadian Hydrographic Service, Québec Region, and the Transportation and Developement Centre, Transport Canada. Their support is gratefully acknowledged.

DEDICATION

I would like to decicate this thesis to my parents Gerald and Delores Townsend.

TABLE OF CONTENTS

LIST OF TABLES

LIST OF FIGURES

LIST OF SYMBOLS, ABBREVIATIONS, AND ACRONYMS

ϕ	-	Latitude.
λ	-	Longitude or wavelenght.
ARNAV	-	Area Navigation.
ASF	-	Additional Secondary Factor.
CLC	-	Calibrated LORAN-C.
DGPS	-	Differential GPS.
DLC	-	Differential LORAN-C.
GPS	-	Global Positioning System.
DSNR	-	Delta-SNR.
DTD	-	Delta-TD.
ECC	-	East Coast Canada LORAN-C Chain.
ECD	-	Envelope-to Cycle Difference.
ED	-	Emission Delay.
FS	-	Field Strength.
GRI	-	Group Repitition Interval.
HDOP	-	Horizontal Dilution of Precision.
LF	-	Low Frequency.
LOP	-	Line-Of-Position.
LORAN	-	Long Range Navigation.
LORCAL^2	-	LORAN-C Calibration at The University of Calgary.
N_{atm}	-	Atmospheric Noise.
NEUSA	-	North East U. S. A. LORAN-C Chain.
NOCUS	-	North Central U. S. LORAN-C Chain.
PF	-	Primary Factor.

PLC - Power Line Carrier.

PPS - Pulse Per Second.

RF - Radio Frequency.

RMS - Root Mean Squared.

S - Siemen (= mho = ohm^{-1}).

SA - Selective Availability.

SF - Secondary Factor.

SGPS - Single Point GPS.

SNR - Signal-to-Noise Ratio.

TD - Time Difference.

TOA - Time-of-Arrival.

WCC - West Coast Canada LORAN-C Chain.

UHF - Ultra High Frequency.

CHAPTER 1
INTRODUCTION

1.1 Background

Recently, two powerful navigation systems have become available for vehicular navigation on a continent wide basis. Loran-C, thanks to the U.S. mid-continent expansion completed in 1991, provides coast-to-coast coverage within much of the populated areas of southern Canada. The Global Positioning System (GPS), a satellite-based system developed by the United States, is designed to provide worldwide navigation. Already in widespread use, it is expected to reach full operational status within months.

Evolving from WW II technologies and developed in the 1950's and 60's, LORAN-C was adopted by Canada and U.S.A. in the 1970's as the primary navigation system for the Great Lakes and the contiguous waters off the coast of North America. In the late 80's, the U.S. Department of Transportation decided to expand LORAN-C in North America to extend its coverage inland and fill the mid-continental gap between the Pacific and Atlantic Coasts. The purpose was to facilitate aircraft Area Navigation (RNAV) and non-precision approaches to airports. This decision practically ensures the continued operation of LORAN-C in the U.S.A. and Canada for decades to come [Lachapelle and Townsend, 1990]. On a global scale, LORAN-C expansion is being considered in many areas of the world. For example, current plans in Europe may see the whole of north-west Europe covered from the Bay of Biscay to the Arctic Ocean [Forssell, 1991].

Figure 1.1 shows LORAN-C coverage in North America [Lachapelle et al, 1992]. The differently shaded area in the central region of the map shows the increase in

coverage made possible by the new U.S. mid-continent LORAN-C expansion. Notice that, with the new coverage, most of Canada's transportation network is covered and this opens the possibility of using LORAN-C for vehicle location on roadways and waterways from coast to coast.

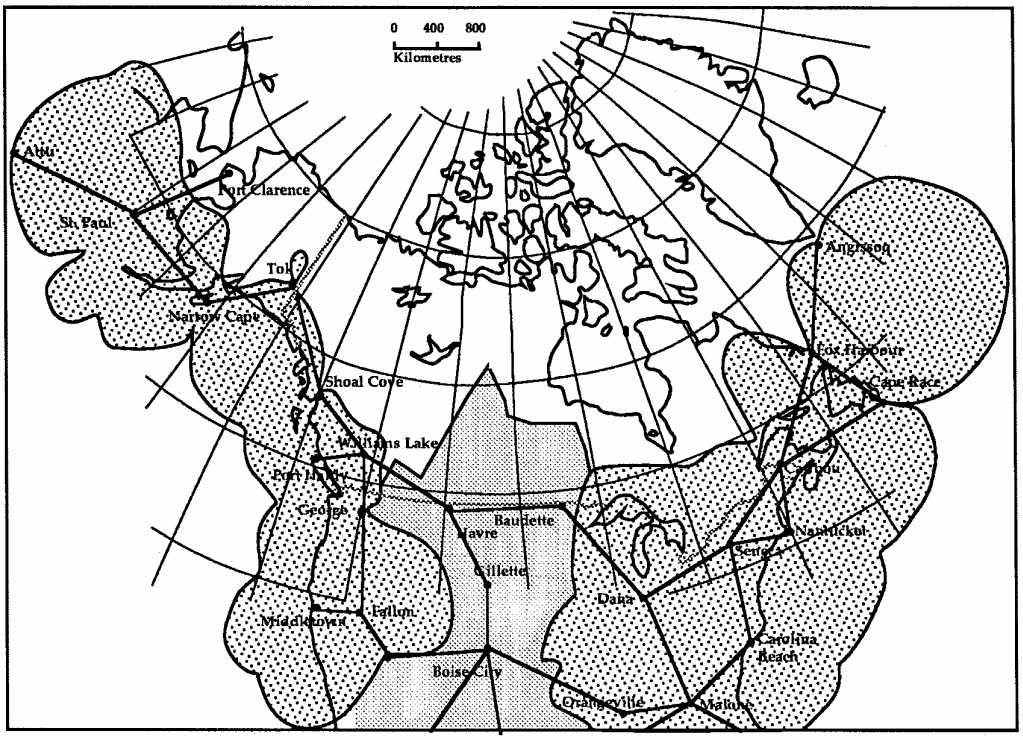

Figure 1.1: Loran-C Coverage in North America Using Single Chain Receivers

GPS is a universal and all weather system which can accommodate a limitless number of users from pole to pole. The L band frequency used by GPS requires line-of-sight propagation but minimizes the effects of weather to provide a high and near-uniform level of accuracy. A complete GPS constellation consists of 21 satellites plus three active spares deployed in six orbital planes 20,000 km above the Earth as shown in Figure 1.2 [Wells et al, 1986]. The observation of at least four satellites simultaneously is sufficient to solve the user's three-dimensional

coordinates. The life span of each satellite is estimated at five to seven years with the on-board time and frequency standards being the most likely parts to result in satellite failure. Such failures will result in degraded geometry in specific areas and over specific periods of time. The constellation will be maintained at a minimum of 18 satellites and the overall availability of the system is, therefore, expected to be relatively high.

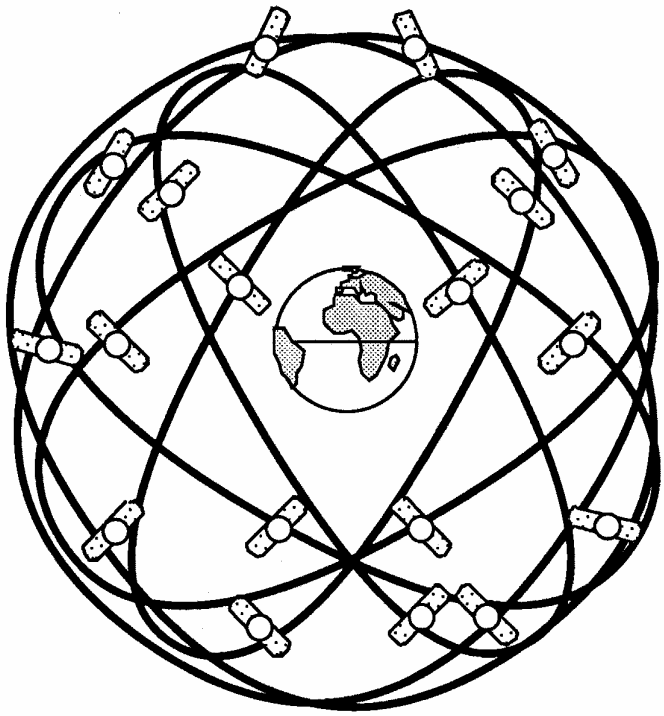

Figure 1.2: Full Constellation of 18 GPS Satellites

1.2 Objectives

For many years LORAN-C has proven itself in a marine environment showing a high level of reliability and a high repeatable accuracy. Using LORAN-C on land is relatively new and its overall performance is not as well known. The signal propagation characteristics are more complicated due to topography, ground

conductivity, and severe seasonal weather variations. GPS signals, on the other hand, are affected differently by these factors. The ground conductivity and weather have little effect while topography will totally block signals causing satellite outages and, therefore, a degradation in navigation coverage.

In considering the problems outlined above, the major objectives of this thesis are as follows:

- Review the LORAN-C system in terms of its operation and performance.
- Discuss the factors affecting the propagation of LORAN-C low frequency (LF) radio waves over land and relate these to LORAN-C accuracy and signal quality.
- Discuss and present methods of improving LORAN-C accuracy through calibration of its measurement biases.
- Present and discuss LORCAL^2 (**LOR**an **CAL**ibration at The University of **CAL**gary), a vehicle-mounted, GPS-based system designed for collecting and analysing LORAN-C data in kinematic mode.

Further objectives of the thesis are realized via case studies of actual LORCAL^2 surveys carried out in various parts of Canada, namely southern British Columbia, the Prairies, and the lower St. Lawrence region of Québec. They are as follows:

- Analysis of LORAN-C signal performance in the regions listed above.
- Compare and analyse various LORAN-C receivers.

- Show the importance of coverage validation with actual field measurements.
- Comparison of performance of LORAN-C and GPS in mountainous regions.
- Investigate the possible advantages of combining GPS and LORAN-C for vehicular navigation.

CHAPTER 2

LORAN-C

2.1 System Description

LORAN-C is a ground based radio frequency (RF) navigation system that operates at a nominal frequency of 100 kHz. It provides two-dimensional (2-D) horizontal positioning (latitude and longitude) to its users twenty-four hours per day and has many marine, air and land applications. The following sections outline several aspects of the LORAN-C system's design and operation.

2.1.1 Low Frequency Radio Wave Propagation

LORAN-C transmitters are located on the ground, and at this low operational frequency (LF), radio waves propagate between the earth and the ionosphere. In Figure 2.1, the direct wave or groundwave, as it is referred to, is shown to propagate along the earth's surface. This property of LF radio waves is due to diffraction caused by the difference in impedance between the earth and the troposphere. The earth has a much higher impedance value than the troposphere.

The ionospherically reflected waves in Figure 2.1 are referred to as the skywaves. The skywaves can make several "hops" between the ionosphere and the earth's surface before reaching the receiver. The multi-hop skywaves are greatly attenuated by the reflection(s) off the earth's surface and, as a result, have much less signal power than the singularly reflected skywave or the groundwave. Therefore, in this thesis the term 'skywave' will be referring to the singularly reflected skywave since it is much more dominant than the multi-hop skywave.

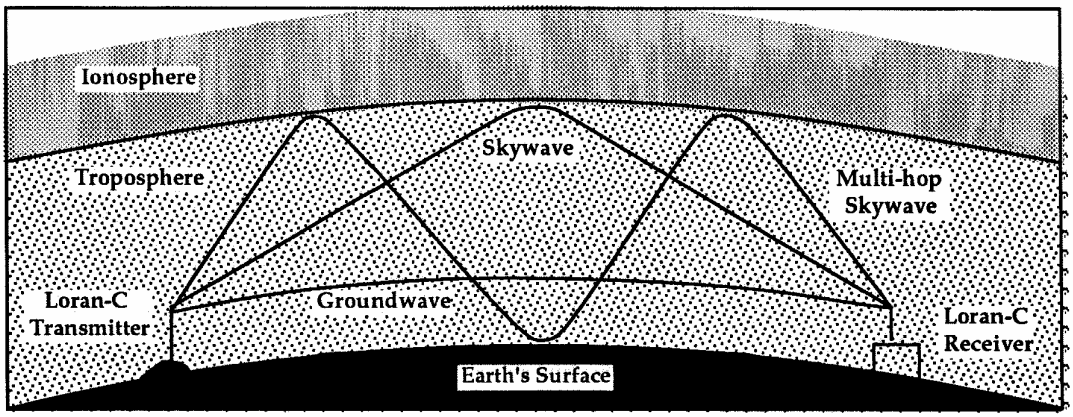

Figure 2.1: LORAN-C Skywave and Groundwave Propagation

2.1.2 Amplitude Modulated Pulse Design

A LORAN-C receiver can track either the groundwave or skywave. The precise path of the ionospherically reflected skywave is not known very well due to fluctuations in the ionosphere. The ideal path of the groundwave is simply the geodesic line between the transmitter and receiver and it can be easily calculated with metre level precision. Therefore, groundwave tracking is always preferred, and required, for most applications. The skywave, however, has a much greater range of reception from the transmitter and, hence, can greatly increase the area of availability if a lower precision is acceptable to the user.

The LORAN-C receiver must distinguish between the groundwave and skywave because anytime a usable groundwave signal is present the corresponding skywave may also be present. To eliminate this ambiguity, the LORAN-C system utilizes an amplitude modulated pulse type signal structure as shown in Figure 2.2. In addition, the pulse rises quickly to allow the receiver to discriminate against the skywave. This is possible because the skywave will always arrive later than the groundwave due to the extra distance it must travel.

Figure 2.3 shows the LORAN-C groundwave pulse in the presence of skywave interference.

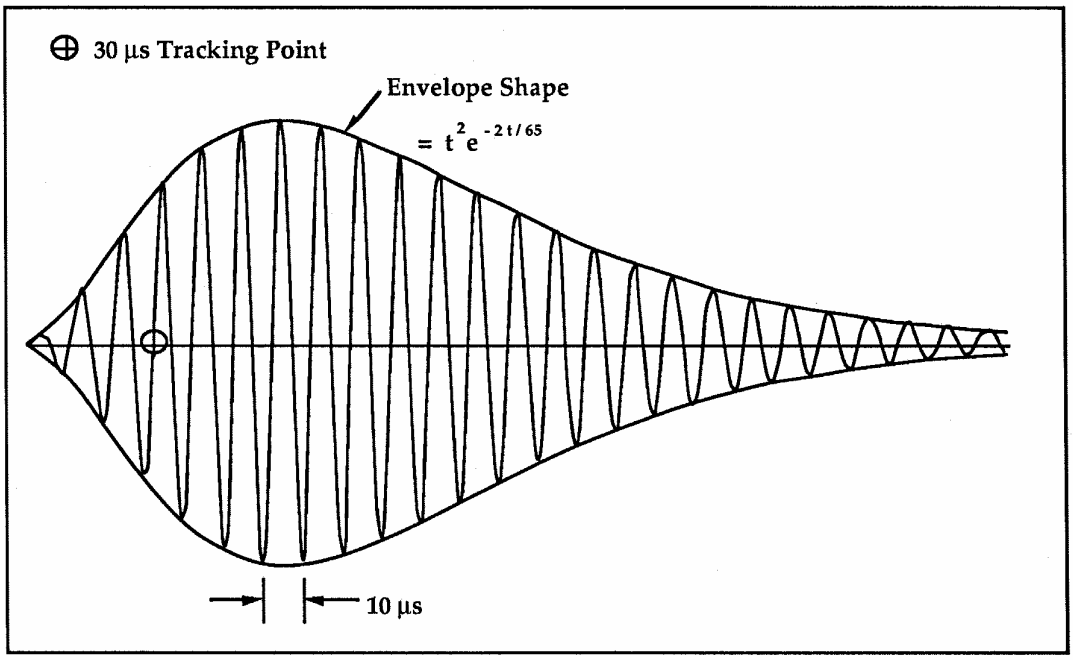

Figure 2.2: LORAN-C Amplitude Modulated Pulse Shape

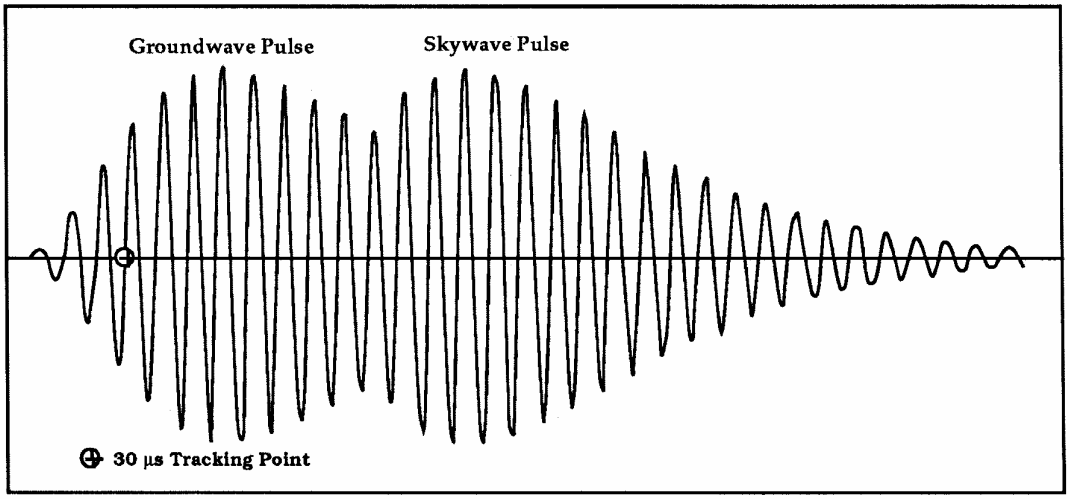

Figure 2.3: Composite LORAN-C Groundwave and Skywave Pulse

The precise tracking point in the pulse is the zero crossing at the end of the third cycle as shown in Figures 2.2 and 2.3. Again, this point is chosen because it is early in the signal and, therefore, resistant to skywave interference. Measurement on a subsequent cycle, e.g., the seventh cycle, is sometimes used for extended air navigation using skywaves. This can increases the range of usage by several hundred kilometres but, as explained earlier, it results in a degraded accuracy and for that reason it is not often used.

The LORAN-C receiver signal tracking process is divided into two sub-processes. In the first process, a coarse measurement called the Envelope-to-Cycle Difference (ECD) is made on the pulse shape to determine the location of the third cycle. This is most important during the signal acquisition stage of receiver operation and it also gives an indication of signal quality by comparing the measured pulse shape with that of the theoretical model. If the pulse is too distorted the receiver will have difficulty and it can result in tracking the wrong cycle. In the second process, a fine measurement is made on the carrier wave to precisely determine the 30 μs tracking point. The measuring accuracy is of the order of 0.01 to 0.1 μs depending on the quality of the receiver and the signal strength. Most receivers require the signal-to-noise ratio (SNR) to be above -10 dB for reliable operation.

2.1.3 Signal Time Sharing Characteristics

A disadvantage of the LORAN-C amplitude modulated pulse is that it occupies a relatively large bandwidth of 20 kHz which makes it susceptible to atmospheric and man-made interference (noise) in the 90 to 110 kHz frequency range. The advantage, aside from the skywave discrimination characteristics discussed

previously, is that every LORAN-C transmitter can broadcast on the same frequency by using time sharing techniques. To illustrate this concept, consider the West Coast Canada (WCC) LORAN-C chain shown in Figure 2.4. The position of these transmitters is designed to maximize navigation coverage along the coast of British Columbia. There are four transmitters designated M, X, Y, and Z, and located at Williams Lake, B.C., Shoal Cove, AK, George, WA, and Port Hardy, B.C., respectively. P is a possible LORAN-C receiver location. The area monitors indicated are required for integrity monitoring of the chain.

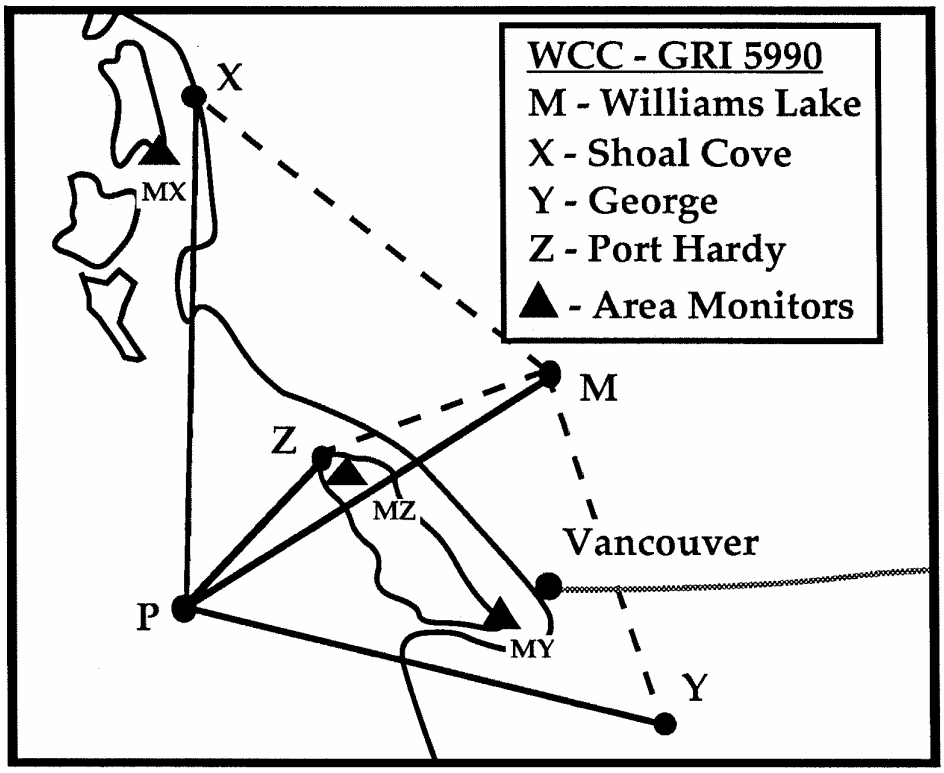

Figure 2.4: West Coast Canada (WCC) LORAN-C Chain

The signal from the master transmitter, M, forms the basis of the signal structure for the chain. The master pulses are transmitted in groups of nine and continuously repeated at a specified Group Repetition Interval (GRI), as shown in

Figure 2.5. The GRI is unique for each LORAN chain and, thus, the receiver can use this to identify which chain it is tracking. The GRI for the WCC is 59900 microseconds (μs). The GRI's for all LORAN-C chains are multiples of 100 and fall within the range of 50,000 μs to 100,000 μs. Normally, the last zero is dropped when the GRI is written. Hence, the GRI for the WCC would normally be written as 5990.

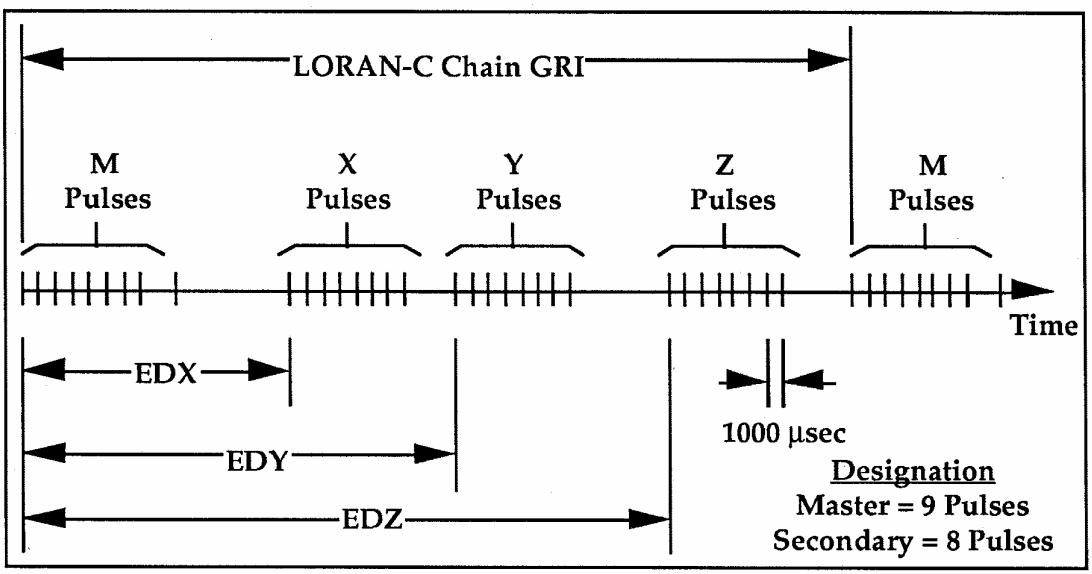

Figure 2.5: LORAN-C Signal Structure

The secondary transmitters X, Y, and Z, (see Figure 2.5) send groups of eight pulses at specified Emission Delays (ED's) from the master group of nine pulses. The ED's are selected such that the signals are received in the same (alphabetical) order throughout the coverage area of the chain. Further, the separation between each ED is at least 10,000 μs to ensure the receiver does not confuse secondaries at times when one or more secondaries are out of range. By design, an ED cannot be longer than the GRI. For example, the ED's for the WCC chain are 13343.60 μs, 28927.36 μs, and 42266.63 μs for X, Y, and Z, respectively. A

LORAN-C chain can have any where from 2 to 5 secondary transmitters and the letter designations range from V to Z.

To obtain useful measurements from this signal structure, the LORAN-C receiver measures the time-of-arrival (TOA) of each group of pulses from the master and secondary transmitters. The TOA of the master is subtracted from the TOA of each secondary to yield time difference (TD) measurements. If the receiver is situated at a location equidistant from the master and a secondary station, the corresponding TD will equal the ED. A difference between the ED and TD will equal the difference in distance from the receiver to the master and secondary stations divided by the propagation velocity of the signals. The distance difference measurements are fed into the navigation component of the receiver to produce coordinates. This process is discussed further in Section 2.1.6.

2.1.4 LORAN-C Autonomous Integrity Monitoring

Figure 2.6 shows a more detailed diagram of the LORAN-C master pulse group. Each pulse is approximately 300 μs in duration and they are transmitted at 1000 μs intervals except for the ninth pulse which is transmitted 2000 μs after the eighth pulse. The secondary pulse group of eight pulses is identical to the master pulse group except that the ninth pulse is omitted. The ninth pulse can be used for identification of the master pulse group by the LORAN-C receiver.

Another important function of the ninth pulse is that it serves as a mechanism to indicate an error in the signal from one or more of the LORAN-C transmitters within a chain. When the area monitors detect a problem in the signal from a given transmitter the ninth pulse is switched on and off in a coded sequence which uniquely defines which transmitter is in error. In addition, the

corresponding secondary transmitter station will 'blink' by turning its first two pulses off and then on for approximately one-quarter of a second every four seconds. The LORAN-C receiver decodes these sequences and warns the user within seconds that there may be a problem. This is especially important in applications where LORAN-C is being used as the primary navigation source.

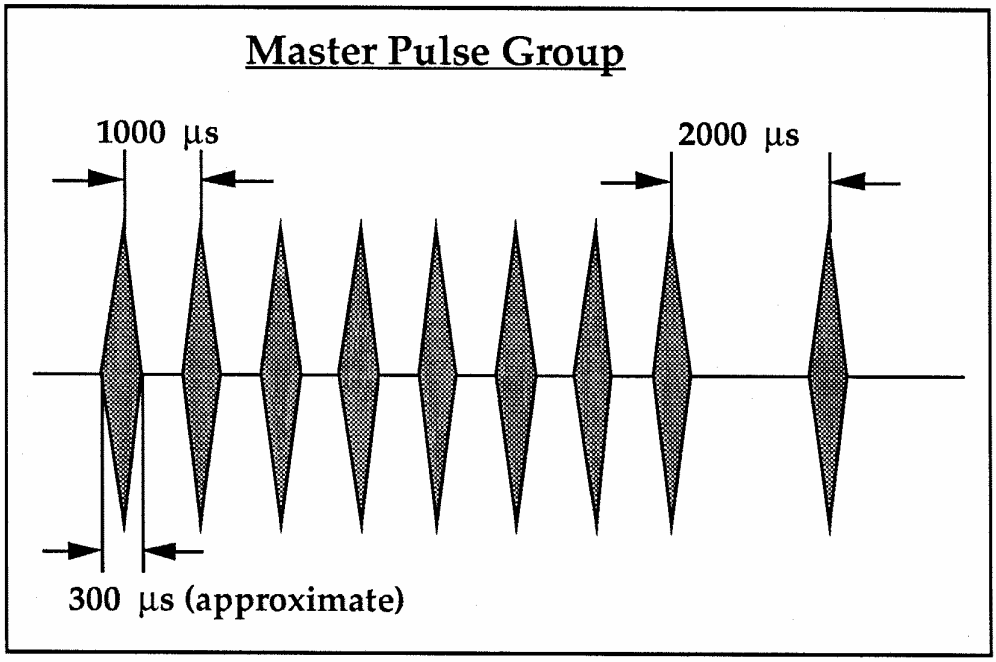

Figure 2.6: LORAN-C Master Pulse Group

2.1.5 Notch Filtering and Phase Coding

As mentioned in Section 2.1.2, LORAN-C is affected by carrier wave interference in the 90-110 kHz band. To counteract this problem, notch filters are implemented in most LORAN-C receivers. A notch filter selectively eliminates the frequencies band(s) of the interfering carrier wave from the incoming signal before it enters the signal tracking component of the receiver. A receiver will typically have two or three notch filters and may have as many as fifteen. The problem with notch filtering is that, with each additional filter, part of the

original signal is lost. Hence, the number filters should be kept to a minimum. The implementation of notch filters can be done with hardware components or digitally with the receiver internal signal processing software.

Phase reversal phase code modulation, illustrated in Figure 2.7, is another aspect of the LORAN-C signal structure which helps it discriminate against carrier wave interference. The alternating A and B sequences over two GRI's spreads the signal power out over the 90 - 110 kHz therby giving LORAN-C additional spread spectrum characteristics.

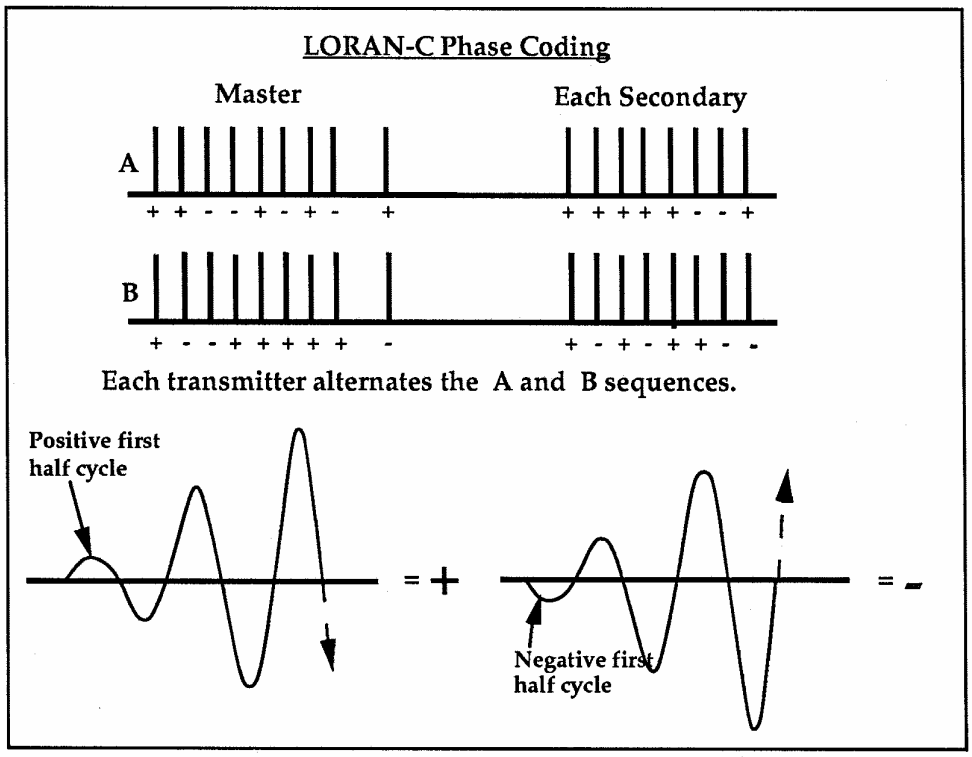

Figure 2.7: LORAN-C Phase Coding

2.1.4 Positioning With LORAN-C

LORAN-C is designed to be used as a hyperbolic positioning system. This is due the fact that a Line-Of-Position (LOP) having a constant TD (or distance difference) with respect to one master-secondary pair of LORAN-C transmitters, will form a hyperbolic line. Signals from two master-secondary pairs will form two hyperbolic LOP's that intersect at a unique position, as shown in Figure 2.8 [CHS, 1983]. Traditionally, in a marine enviroment, a navigator would read the raw TD measurements from the LORAN-C receiver and use the hyperbolic lines already plotted on the nautical chart to derive a position. This is called Chart Latticing.

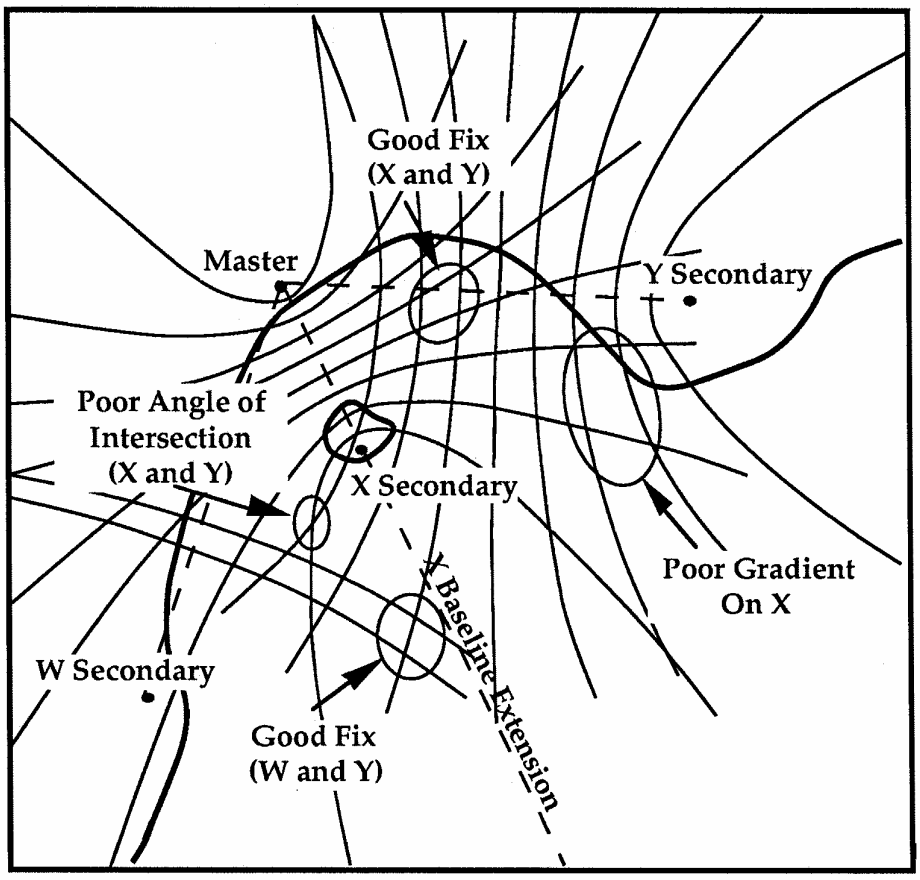

Figure 2.8: Hyperbolic Lines of Position

Modern LORAN-C receivers use the raw TD measurements to compute the latitude and longitude of the receiver antenna position directly using a method such as least squares.

2.2 Error Sources Affecting LORAN-C

The errors affecting LORAN-C can be categorized into time dependent and time independent errors. Time dependent errors are those that vary rapidly with time. Time independent errors are biases that, for all intent and purposes, do not change over time [Lachapelle and Townsend, 1991].

2.2.1 Atmospheric Propagation Delays

As with any other RF system, LORAN-C is affected by the atmosphere. Since the troposphere is a non-dispersive medium in the RF band, its nominal effect on the 100 kHz LORAN-C signal is the same as on any other RF system. However, LORAN-C signals travel along the earth's surface over relatively long distances and the cumulated effect of the troposphere is much larger than that on a satellite based system. The resulting delay is the primary phase lag, or primary factor (PF) as it is also called, which is easily computed if the refractivity N is known:

$$N = f(T, P, e)$$

where T, P and e are the dry atmospheric temperature, atmospheric pressure and partial water vapour pressure, respectively. In practice, average values for T, P and e are used to derive an average N. The use of seasonal or monthly averages is generally sufficient unless large short term variations occur, in which case the use of observed weather data is preferable. This is the case of weather

fronts which, in many cases, can have an effect of 30 to 50 m on a position line as shown in Figure 2.9 [Samaddar, 1980]. Propagation delays which are due to regional weather patterns can be corrected by differential LORAN-C (DLC). The effects of weather fronts will generally be more difficult to remove with DLC unless an adequate weather station network is in place. At sea, where the above atmospheric parameters are more stable, the use of DLC has resulted in performance of better than 20 m [Viehweg et al, 1988].

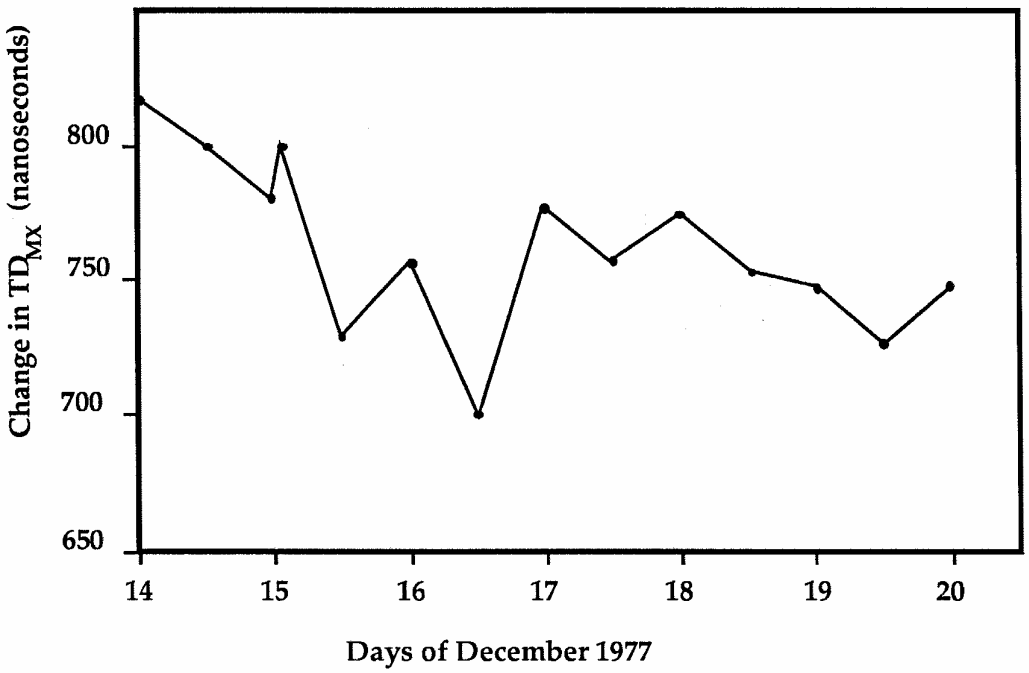

Figure 2.9: Typical Effect of Weather Front on Time Differences

2.2.2 Atmospheric Noise

Atmospheric noise does not affect the propagation speed of the LORAN-C signal but affects its detectable signal and, thus, its range. The LORAN-C signal occupies the 90-110 kHz bandwidth. In this band, RF noise originates from two sources, namely natural (atmospheric) and man-made. Natural sources include

lightning bursts occurring during lightening storms and are seasonal in nature. Man-made noise originates from electrical interference such as Power Line Carrier (PLC) transmitters operating in the same frequency band and other RF sources. This is especially serious in heavily industrialized areas. The average atmospheric noise in Canada and Northern United States is shown in Figure 2.10 [RTAC, 1987].

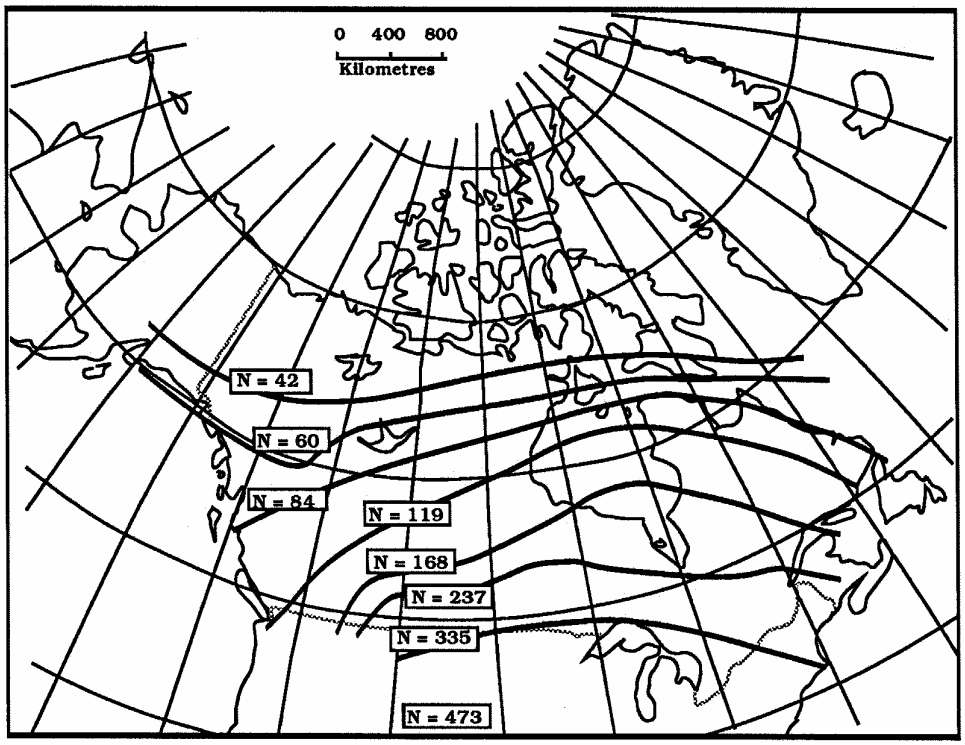

Figure 2.10: Average Atmospheric Noise ($\mu V\ m^{-1}$)in Canada and Northern U.S.A

Seasonal variations can reach 10 to 20 dBs [CCIR, 1988a]. The noise varies from 42 $\mu V\ m^{-1}$ in Northern Canada to 473 $\mu V\ m^{-1}$ in the Northern part of the U.S.A. The LORAN-C signal strength in the latter area would have to be 20 dB above that in Northern Canada to be detectable at a threshold level of -10 dB. As discussed before, notch filters are used in LORAN-C receivers to help limit signal

interference at specific frequencies. The use of too many filters can, however, distort the pulse shape and reduce the receiver measuring accuracy.

A variety of factors such as precipitation static and skywave interference can cause frequent cycle jumps in a LORAN-C receiver. A cycle jump happens when the LORAN-C receiver signal tracking "jumps" away from the third cycle and begins tracking the zero crossing on another cycle. For example, it might jump to the 2nd or 4th cycle.

2.2.3 Ground Conductivity

The ground conductivity affects both the signal strength and the propagation delay of the transmitted signal.

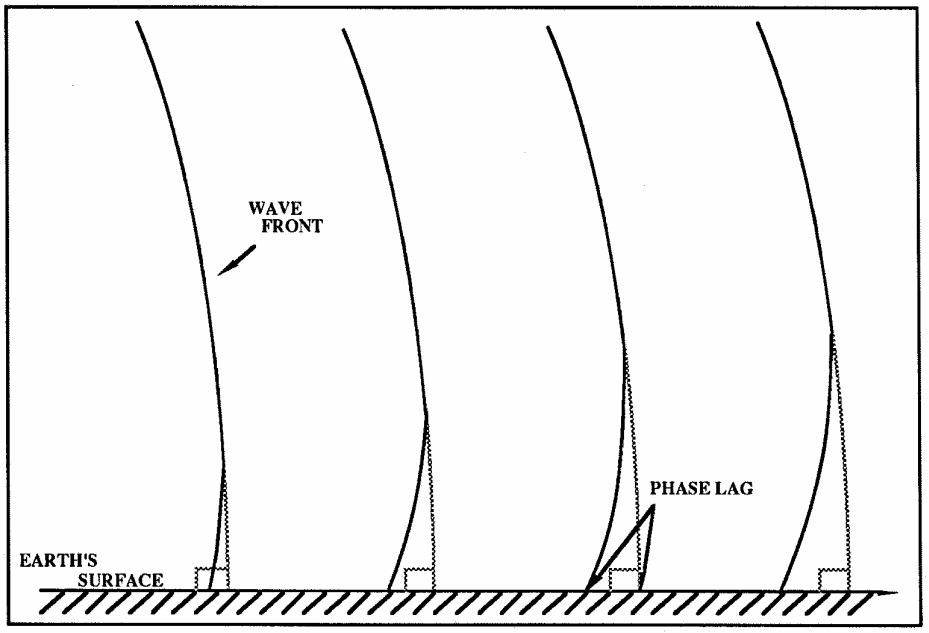

Figure 2.11: Bending of the LORAN-C Wave due to Ground Absorption

The delay due to propagation over sea water is called the secondary phase lag while the additional delay due to propagation over ground is called the

additional secondary phase lag. These are also called the secondary factor (SF) and additional secondary factor (ASF), respectively. Poor conductivity results in increased absorption of the RF wave into the ground and a bending of the wave front as shown in Figure 2.11.

Increased absorption results in a more rapid attenuation of the signal. The phase lag increases with distance from the transmitter and decreases with increasing conductivity. It is maximum on the ground and generally decreases to zero at approximately 5 signal wavelengths above the ground.

This means that the LORAN-C calibration for surface users should be made on the ground while calibration for airborne users should be made at flight altitude. Sea water is the best Earth's surface conductor with a conductivity of 5 S m^{-1} while salt free ice is worst at 10^{-5} S m^{-1} (S = Siemens). Cities, with large concrete and asphalt surfaces, are considered to be poor conductors. The field strength (FS) and, therefore, the effective range of the LORAN-C signal is affected by conductivity as shown in Figure 2.12 where three types of surface and a nominal transmitter power of 400 kW are illustrated.

The correction table for higher and lower transmitter powers shows that increasing the transmitter power by a factor of four, namely to 1600 kW, increases the signal strength by 6 dB. The conductivity can, in certain cases, be affected by seasonal variations. A dry season followed by heavy rains which result in a large water content difference in the soil will affect the conductivity significantly. Snow coverage will, in itself, have a limited effect on conductivity variation since absorption of the transmitted signal at LORAN-C frequency takes place over a depth of between 10 and 100 m below the earth's surface. The ASF

can, therefore, be considered constant in time and can be calibrated. DLC would assist marginally in removing the effect of conductivity variations and cannot be considered a viable solution for land users.

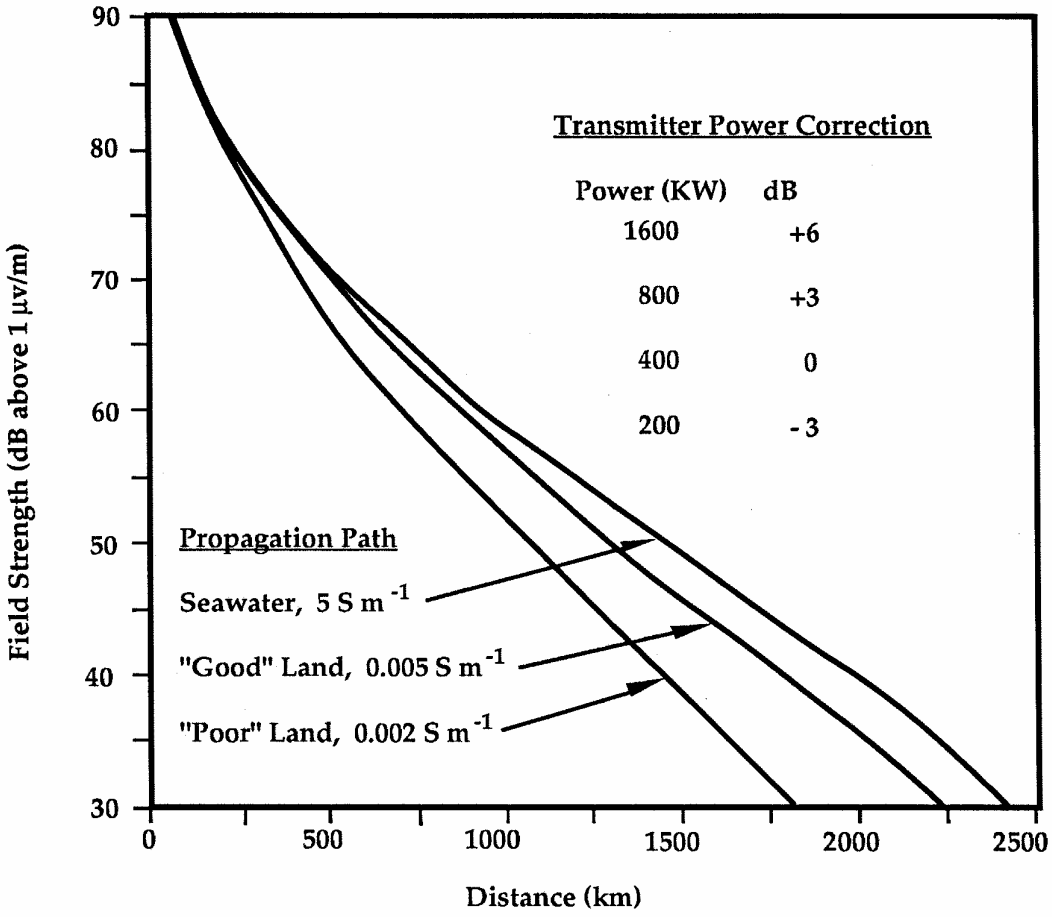

Figure 2.12: LORAN-C Field Strength Prediction Chart

2.2.4 Topography

The effect of rugged topography on LORAN-C signal propagation is complex and results in an ASF which is very local in nature and can reach several hundred metres at ground level [Samaddar, 1980]. An example of the combined secondary and additional secondary phase lags along a profile crossing the

Aleutian Islands, a mountainous region of Alaska, is shown in Figure 2.13 [Johler and Cook, 1984].

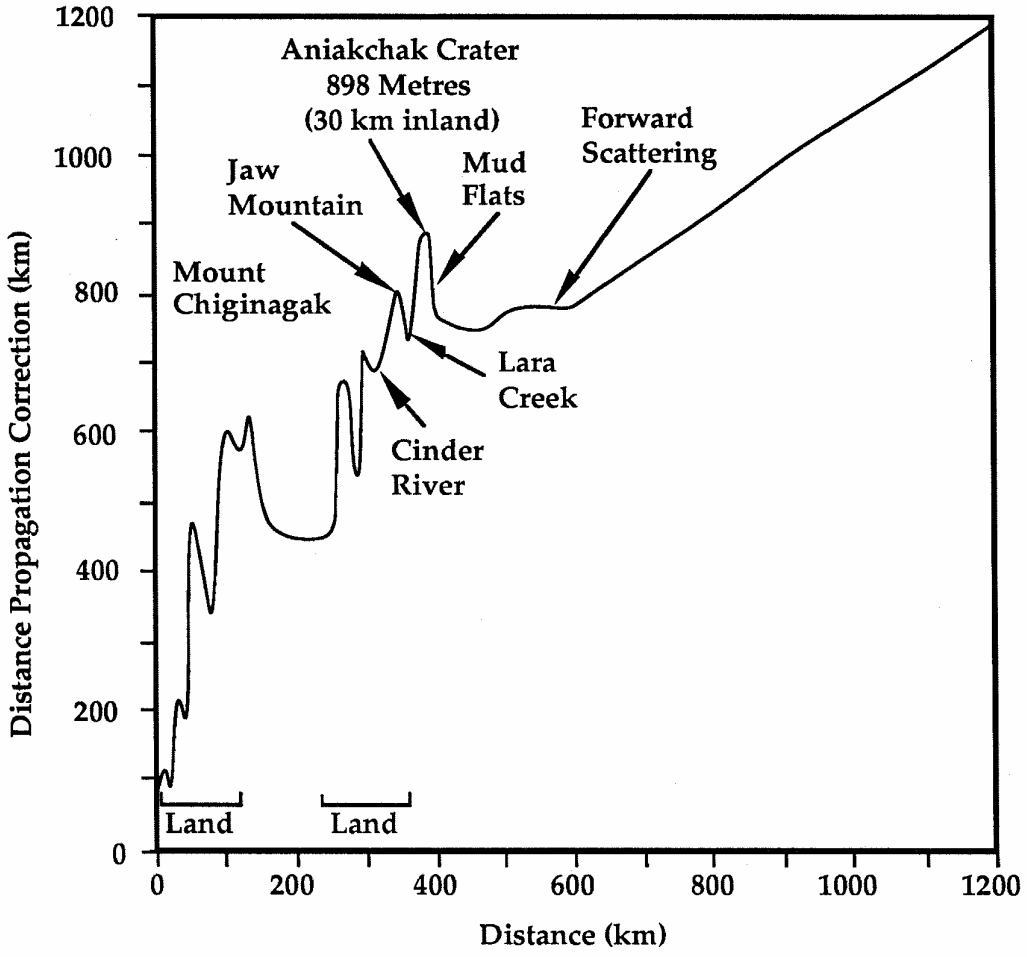

Figure 2.13: Combined Effect of Secondary (Conductivity) and Additional Secondary (Topography) Phase Lags along a Selected Profile of the Aleutian Islands

The local variations are largely caused by the topography. Such variations are also encountered in the Western Cordillera of Canada and the United States as will be seen later. The additional secondary phase lag is also constant in time and can be calibrated together with the secondary phase lag. It may be difficult to separate the two effects unless detailed conductivity measurements are available

but this difficulty is transparent to the user. Thus, DLC will not contribute to the removal of the additional secondary phase lag in view of its local nature.

2.2.5 Altitude Effects

At flight altitude, two effects are different than those on the ground below, as shown in Figure 2.14. Firstly, the additional secondary phase lag is attenuated with altitude as discussed earlier. Secondly, the LORAN-C signal travels along the curved earth's surface until a point at which the aircraft is in the line-of-sight. The signal then propagates to the aircraft along a straight line. The conductivity and topography affect the signal only during the travel along the earth's surface. The predicted total altitude effect for an aircraft located some 360 km from a transmitter is shown in Figure 2.15 for five hypothetical conductivity values of the ground [Moussa, 1990].

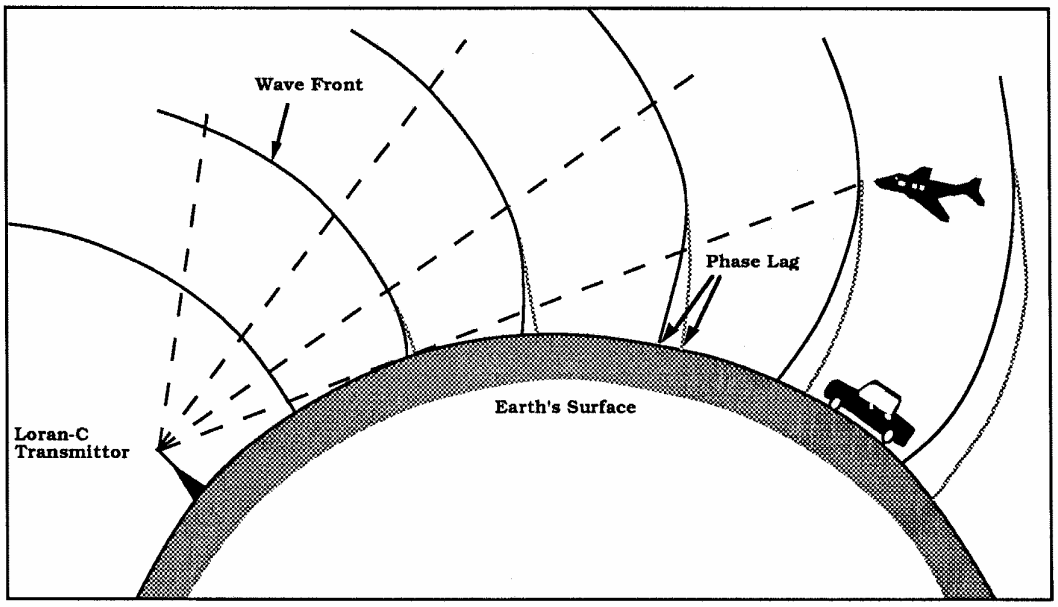

Figure 2.14: Effect of Altitude on LORAN-C Wave Front

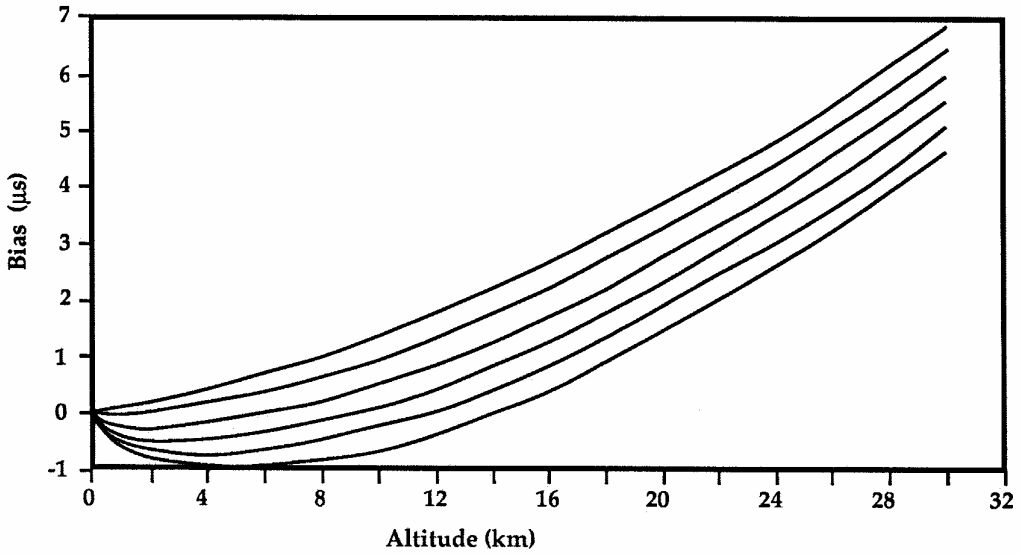

Figure 2.15: Effect of Altitude and Ground Conductivity on the LORAN-C Signal For An Aircraft 360 km From the Transmitter

2.2.6 System Effects

The errors due to system effects include the instabilities of the transmitted signals, receiver noise, and hyperbolic geometry. The transmitters local atomic time and frequency standards are controlled through a monitor located within the chain coverage. This error source is estimated to be well below 20 m. The measuring accuracy of a LORAN-C receiver is a function of its components and varies between 5 and 30 m. The effect of hyperbolic geometry was discussed briefly in the Section 2.1.4. The magnitude of this effect is purely a function of the geometry between the user and the transmitters in use. With the availability of low cost multi-chain receivers, the accuracy degradation due to the system geometry is expected to decrease significantly in many parts of North America. While the effects of the transmitters clocks and receiver noise are time dependent, the effect due to the geometry is constant in time for a given location and a given configuration of transmitters.

2.2.7 LORAN-C Stability

It has been shown that the stability of LORAN-C signals is a function of several time dependent parameters, namely atmospheric propagation delays, atmospheric noise and system effects. Typical signal stability, in terms of derived position variations, is shown in Figure 2.16 for a station located at Pemberton, 90 km north of Vancouver, B.C. [Lachapelle et al, 1989].

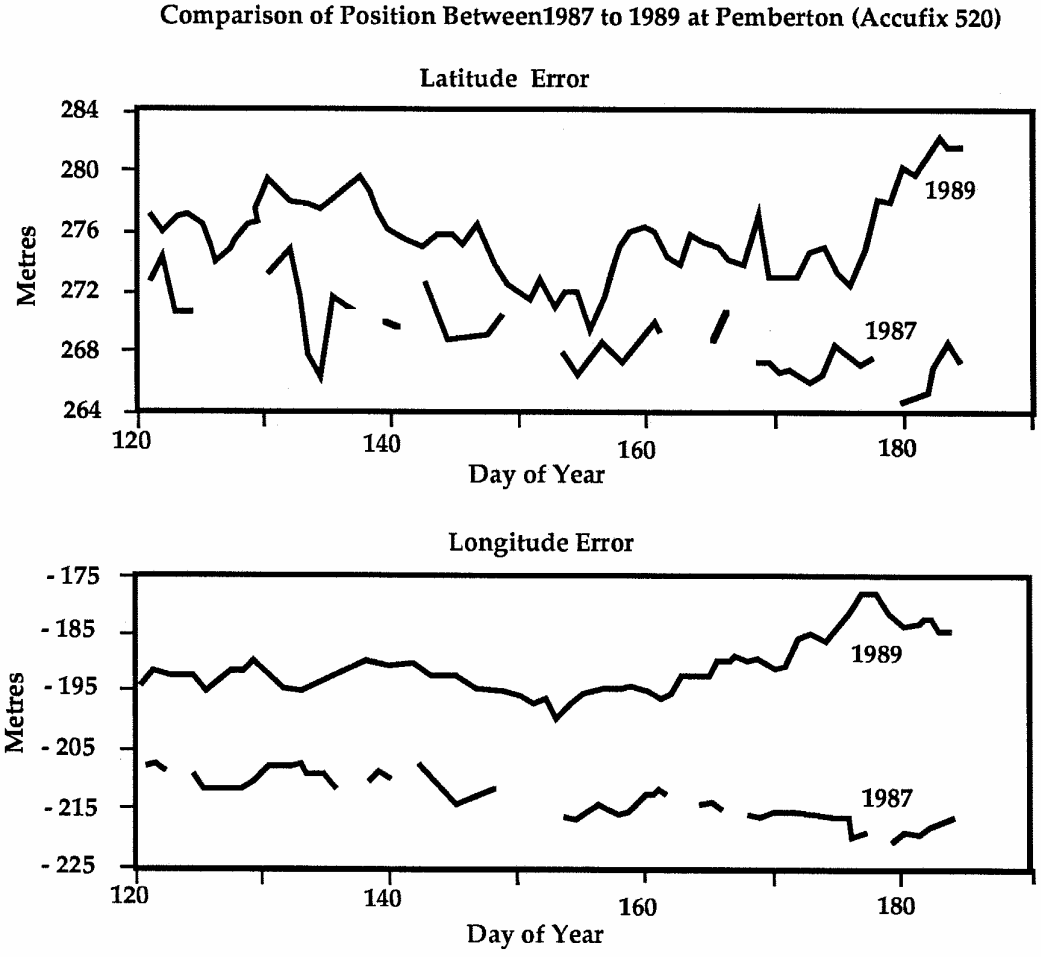

Figure 2.16: LORAN-C Long Term Stability (1987 - '89) - West Coast Canadian Chain

LORAN-C data was gathered with a Megapulse Accufix 500 LORAN-C receiver during May and June of 1987 and 1989, respectively. The atmospheric conditions were relatively stable and similar during these two periods. The differences in each of the two horizontal components between the two periods are less than 30 m, which is below the maximum values anticipated from the two remaining time dependent error sources.

receiver distance from the transmitter for several conductivity values using a spherical earth model [Johler et al, 1956].

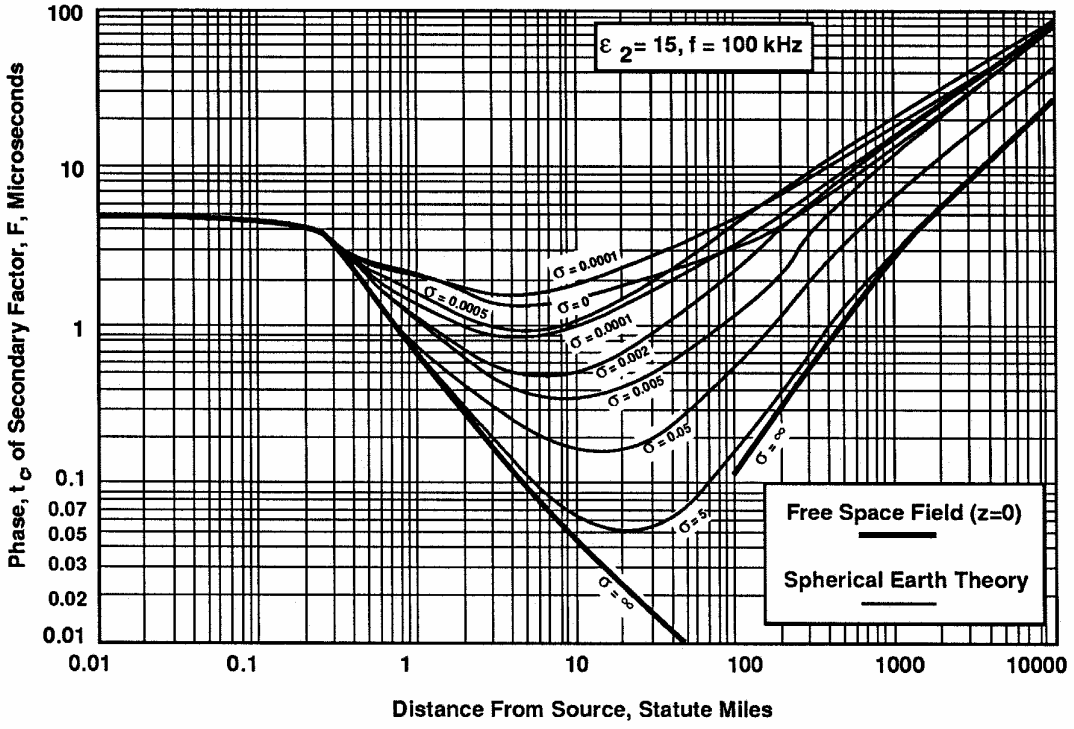

Figure 3.1: Phase of Secondary Factor With Distance From Source For Various Conductivity's

Equations for the ASF attempt to model the effects due to variations in conductivity and terrain along the propagation path between a transmitter and receiver. The Millington-Pressy method was one of the first to address the problem of conductivity variations [Samaddar, 1979]. They approximated the propagation path between the transmitter and receiver by dividing it into several shorter paths according to the variation in conductivity values. The phase lag or impedance for each smaller section is calculated then added together for the overall (cumulative) phase lag. For example, the signal from a transmitter

located some distance inland is being received by receiver on a ship at sea. The propagation path would naturally be divided into two sections; i.e. the over land path and the over sea path because the sections will almost certainly have large differences in conductivity. Hence, the method works well as long as there are clearly discernible segments along the propagation path. The method does not, however, take into account any terrain variations and, therefore, produces poor results in rugged terrain.

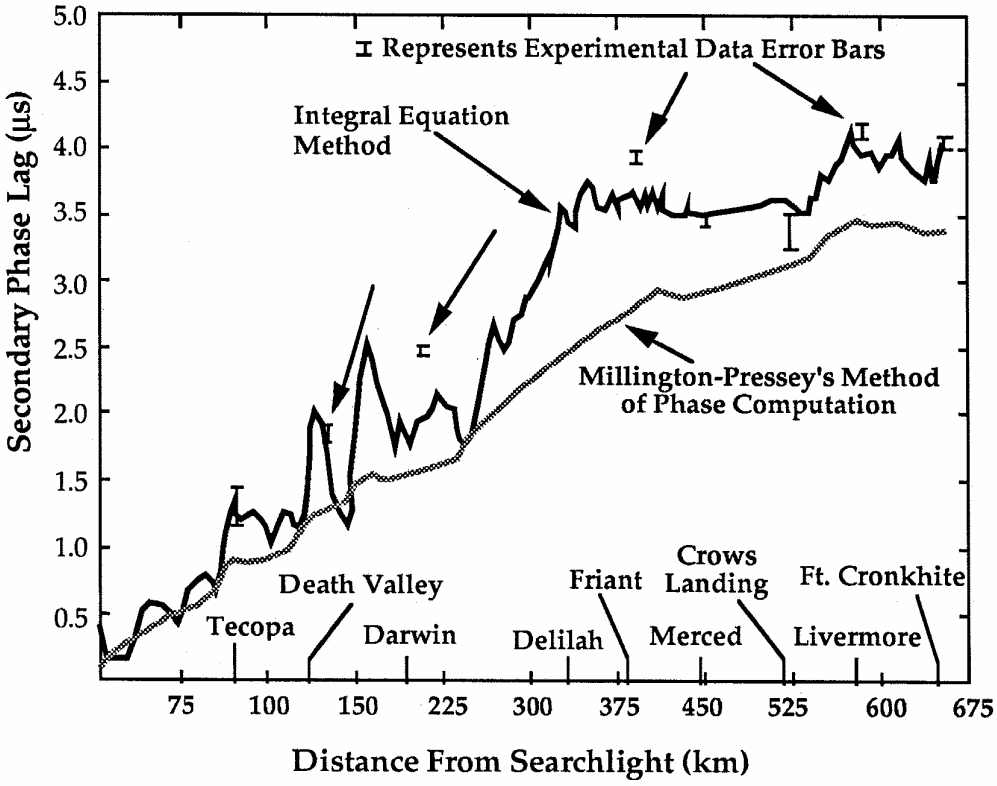

Figure 3.2: Comparison of Predicted Results From Integral Equation and Millington-Pressey's Methods to Measured Experimental Data

One such method that does take into account the variations in terrain, is the integral equation approach developed by Hufford [1952] and furthered by Johler

[1977]. Figure 3.2 shows a comparison of predicted results from the integral equation and Millington-Pressey's methods [Samaddar, 1979]. The integral equation method shows significantly better results than Millington-Pressey's method but still disagrees with the measured data by as much as 0.5 μs (150 m) which is significantly worse than what could be achieved in terms of the repeatability shown in Section 2.2.7. In any case, these methods require precise knowledge of the ground conductivity and topography along the propagation path to produce accurate results.

3.2 Calibration of LORAN-C Using GPS

The concept of calibrating LORAN-C derived positions with GPS is straightforward. LORAN-C derived horizontal position components are compared with corresponding GPS-derived components. The differences are due to the time dependent and time independent LORAN-C measurement biases, as described in the previous chapter, as well as errors in the GPS derived positions. If one assumes that the predictable regional weather patterns are accounted for, the remaining combined time dependent effects on the LORAN-C position is well below 50 m. The remaining time independent effects are large but constant. Differential GPS (DGPS) can yield an instantaneous position accuracy of ≤ 5 m in either static or kinematic mode. Therefore, by comparing the LORAN-C position with the DGPS position, the resulting time independent effects on the LORAN-C position can be estimated with an accuracy of 50 m or better.

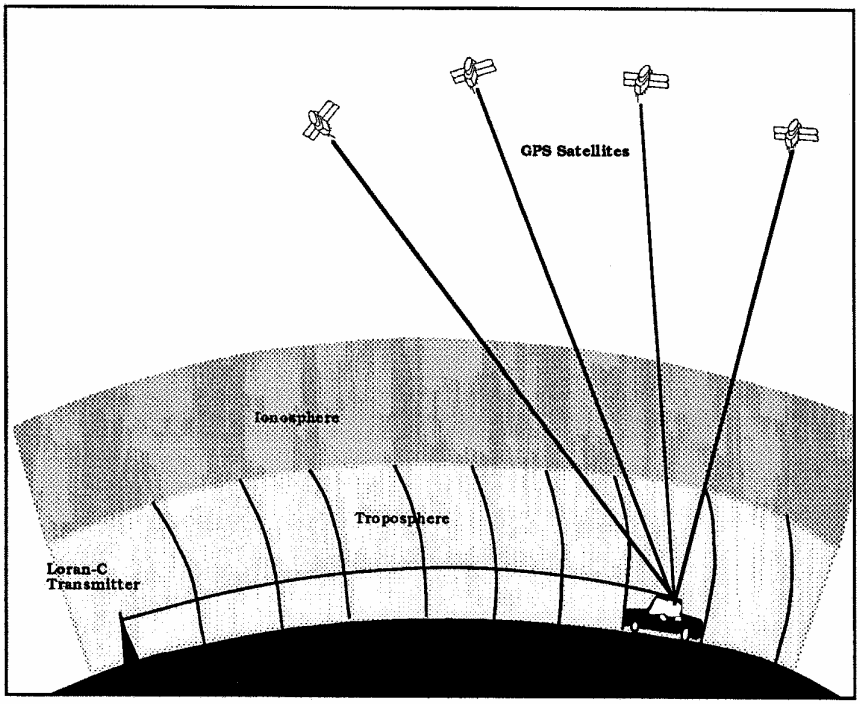

Figure 3.3: LORAN-C versus GPS

Some relevant differences between LORAN-C and GPS characteristics are shown in Figure 3.3 and summarized in Table 3.1. Although the effect of the troposphere is nominally the same for both, the cumulative effect on LORAN-C is much larger since the signals travel through several hundred km of troposphere along the earth's surface as opposed to 60 to 80 km for a GPS signal received from a satellite located at the zenith. The GPS signal is, however, delayed by the ionosphere and the LORAN-C signal is not. Effects due to conductivity, topography and atmospheric noise are significant on LORAN-C while practically insignificant on GPS. The measurement resolution of the GPS C/A code is higher than that on the LORAN-C amplitude modulated pulse. The hyperbolic mode used currently for most LORAN-C applications is subject to more rapid degradation than the GPS in pseudorange mode. The use of the

pseudorange mode with LORAN-C may, however, become widespread with the availability of multi-chain receivers and this would improve its positioning geometry.

Table 3.1: Major GPS and LORAN-C Characteristics in the Context of Vehicular Navigation

GPS (UHF, 1.5 GHz)

1. Line-of-sight propagation.
2. Short tropospheric path.
3. Affected by the ionosphere.
4. Not significantly affected by ground conductivity or atmospheric and man-made noise.
5. Signals blocked by topography and structures.
6. High measurement resolution (≤ 1 m).
7. Absolute accuracy: 100 m under SA (Selective Availability).

LORAN-C (LF, 100 KHz)

1. Propagation along earth's surface.
2. Line-of-sight not required.
3. Effects of refractivity (PF), ground conductivity (SF + ASF), topography and atmospheric or man-made noise are significant..
4. Lower measurement resolution (10 - 30 m).
5. Poor geometry in many areas.
6. Absolute accuracy: ≤ 500 m nominal, 100 m calibrated (for permanent distortion effects).

The nominal horizontal accuracy of LORAN-C is stipulated currently at 500 m while that of GPS is at 100 m with Selective Availability (SA) implemented. However, if the LORAN-C errors due to the time independent effects of conductivity and topography can be effectively calibrated with GPS as described above, this would increase the positioning accuracy of LORAN-C to near that of GPS with SA on [Lachapelle and Townsend, 1990].

3.3 Calibration at Discrete Points

The use of GPS to analyse local variations of the combined effects of conductivity and topography was tested in the Summer of 1989 in an area surrounding Pemberton Airport, approximately 90 km North of Vancouver, B.C. [Lachapelle et al. 1989]. Eleven stations within a radius of 80 km from Pemberton Airport were selected as shown in Figure 3.4. A static differential GPS survey of all sites was conducted to obtain accurate WGS72 horizontal coordinates for all stations. At the time, WGS72 was the reference system used for all LORAN-C chains in North America. It has since switched over to WGS84. The heights of the stations vary from 200 to 1,000 m and surrounding mountains reach an elevation of up to 3,000 m. The airport station at Pemberton was occupied permanently for nearly one year while the remaining 10 stations were each occupied for a 24-hour period. TD's from the following three transmitters, which are part of the West Coast Canadian Chain, were recorded: M (Williams Lake), Y (George, Washington) and Z (Port Hardy).

The latitude and longitude differences between LORAN-C derived and GPS derived WGS72 coordinates are also shown in Figure 3.4.

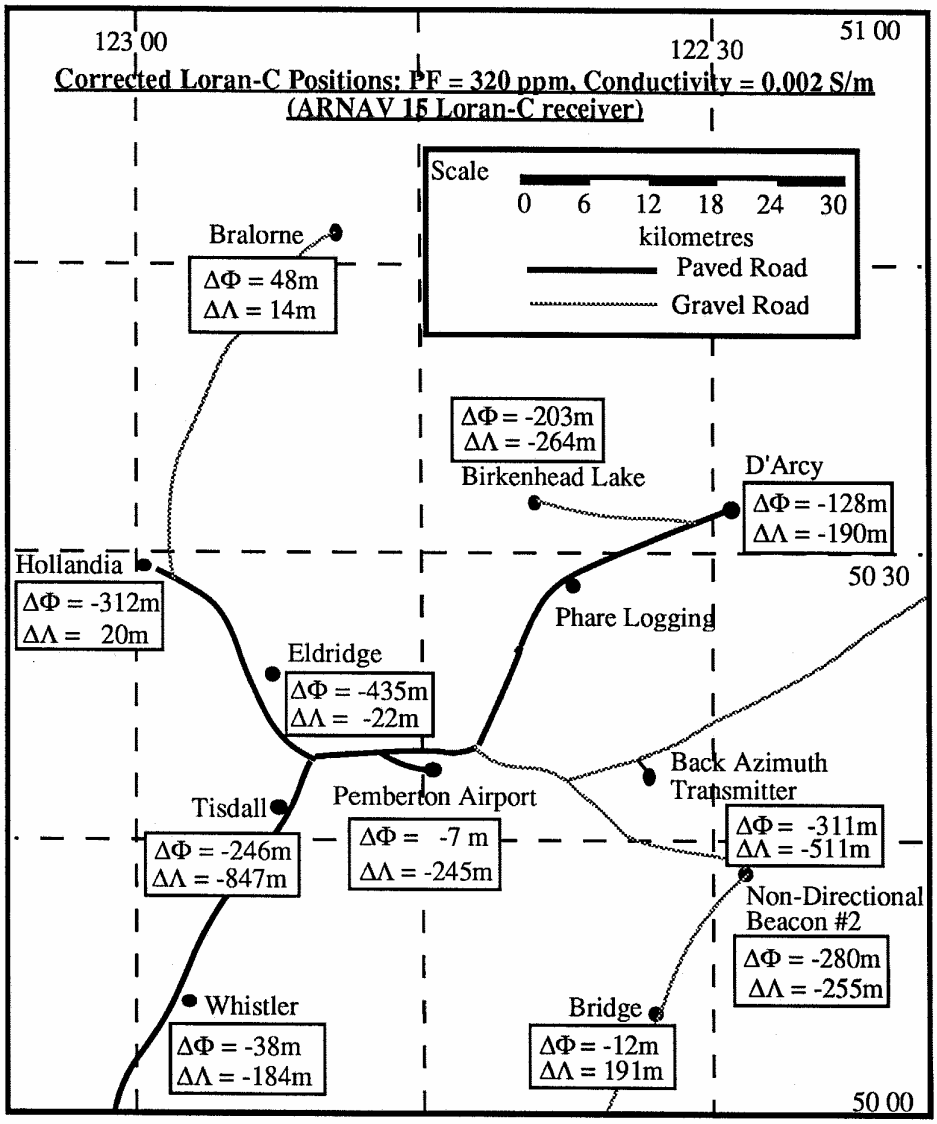

Figure 3.4: Absolute Accuracy of LORAN-C at Remote Stations

The LORAN-C TD measurements were corrected for the propagation effects with a PF of 320 ppm and a combined SF and ASF of 0.002 S m^{-1}. The estimated variations in latitude range from -435 m for Eldrigde to 48 m for Bralorne while those in the longitude range from -847 m for Tisdall to 191 m for Bridge. Back Azimuth and Bralone are approximately 40 km apart while Tisdall and Bridge

are approximately 40 km apart also. These anticipated large distortions are caused by the topography as discussed earlier in Chapter 2.

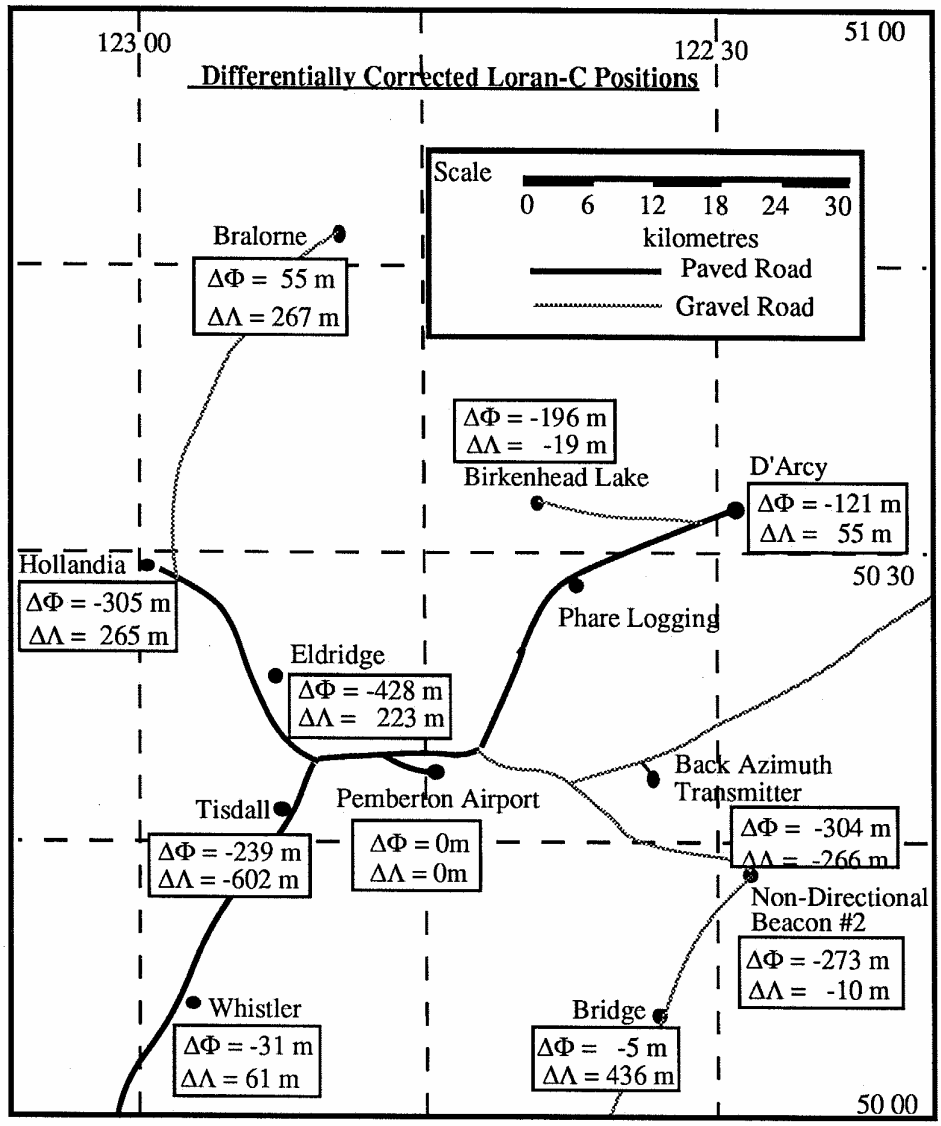

Figure 3.5: Residual Errors in Differentially Corrected Loran-C Coordinates

Figure 3.5 shows the differences between differentially corrected LORAN-C and GPS-derived WGS72 coordinates at the 10 remote sites. The differentially corrected LORAN-C positions were obtained by applying the position

differences (LORAN-C minus GPS) obtained at the airport to all remote stations. This is why the differences at the airport site are zero.

Evidently, the use of differential LORAN-C in a mountainous area such as that around Pemberton will not improve results substantially. The time-dependent variations which are reduced through the use of differential techniques are much smaller than the time-independent but position-dependent variations caused by the rapidly changing effect of the topography.

Although the effects are large and outside the 500 m (2-D rms) accuracy prescribed for LORAN-C marine areas, they are constant in time and need to be calibrated only once. The rapid variations as a function of distance, however, preclude the use of effective interpolation techniques based on point values. The use of continuous profiles along the roads or routes of interest is, therefore, required. Results from a GPS-based LORAN-C calibration system along continuous profiles is discussed in the next section.

3.4 Enroute Calibration of LORAN-C

A continuous profile along the 30 km road between Hollandia and Pemberton Airport was measured with LORCAL^2 (**LOR**an **CAL**ibration at The University of **CAL**gary) in February 91. The LORCAL^2 system was designed by the author to collect and process GPS and LORAN-C data along continuous profiles in kinematic mode. LORCAL^2 will be discussed in detail in the next chapter. For this test, the LORAN-C receivers selected consisted of an Accufix 520 and LocUS Pathfinder units. The Accufix 520 is an upgrade to the 500 unit used at Pemberton during the 1989 field campaign. While the Accufix 520 is based on analog technology, the Pathfinder is a prototype digital unit which measures the

same quantities as the Accufix 520 [Post, 1989]. Both are single chain units. GPS is used in differential mode to provide reference positions of the vehicle with an accuracy better than 10 m.

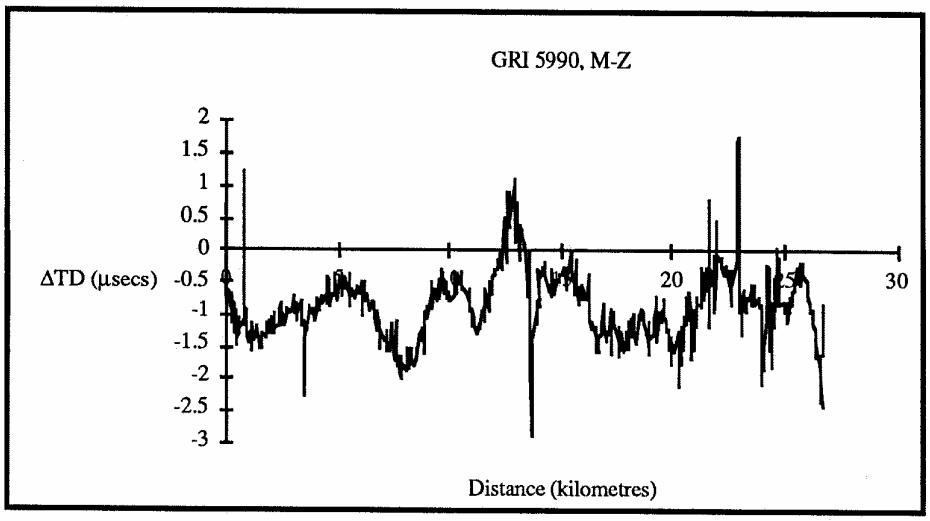

Figure 3.6: Residual Time Differences Between Stations Hollandia and Pemberton Airport (PF = 320 ppm, Conductivity = 0.002 S m^{-1})

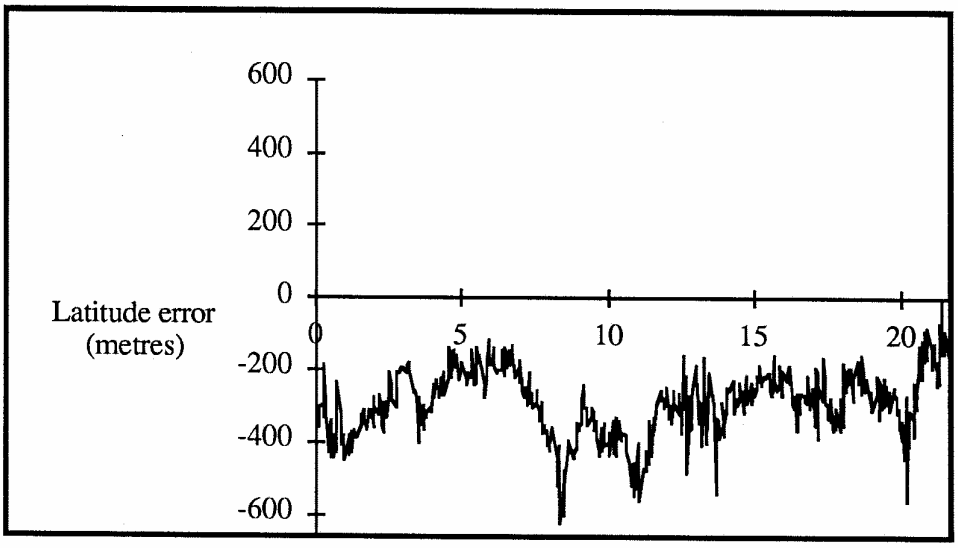

Figure 3.7: Latitude Error - En-Route Calibration of LORAN-C with GPS Between Stations Hollandia and Pemberton Airport

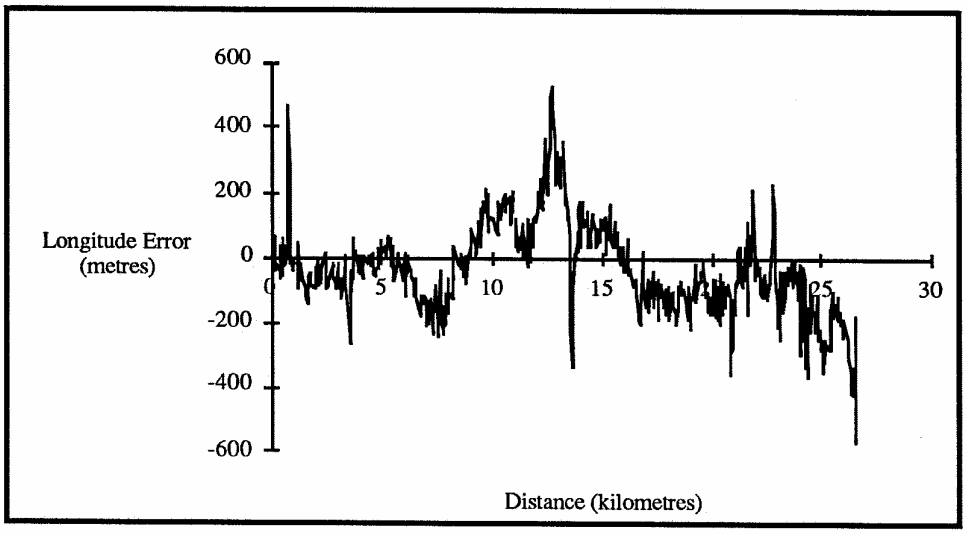

Figure 3.8: Longitude Error - En-Route Calibration of LORAN-C with GPS Between Stations Hollandia and Pemberton Airport

The variations in the TD from Port Hardy (Z) along the profile are shown in Figure 3.6. The latitude and longitude errors are shown in Figures 3.7 and 3.8, respectively [Lachapelle et al,1992c]. TD variations over distances of a few kilometres exceed 2 μs (i.e., 600 m) and are the cause for the corresponding variations of up to several hundred metres in the position components. The agreement with the distortions previously determined at Hollandia and Pemberton Airport (Figure 3.4) is of the order of 30 to 50 m, which is within the repeatable accuracy anticipated for LORAN-C. These en-route variations are due to the surrounding topography. The magnitude of the distortions is in agreement with results obtained by other investigators [e.g., Johler & Cook, 1984]. Also, as pointed out earlier, the effect of the topography on phase distortion can be predicted using appropriate data but the complexities are significant [Samaddar, 1979]. Enroute calibration using LORCAL^2 porvides a practical alternative.

CHAPTER 4

THE LORCAL^2 SYSTEM

4.1 Introduction

The LORCAL^2 (**LOR**an **CAL**ibration at The University of **CAL**gary) system was designed by the author to collect and process GPS and LORAN-C data along continuous profiles in kinematic mode. It may be used in land, air, or marine mode. The primary focus in the design of LORCAL^2 was to build a system for LORAN-C calibration [e.g. Lachapelle and Townsend, 1991], but it has since proven to be a valuable tool for a variety of other investigations involving LORAN-C and GPS . These include LORAN-C signal analysis and coverage validation [e.g. Townsend et. al., 1992a, Lachapelle et al, 1993b], LORAN-C receiver comparisons, and hybrid GPS/LORAN-C [Lachapelle and Townsend, 1993]. Chapters 5 will demonstrate these applications in the form of case studies of actual field campaigns. The following sections in this chapter will focus on the design and performance of LORCAL^2.

4.2 LORCAL^2 Hardware Configuration

The LORCAL^2 system is designed to be a flexible tool and as a result it can be configured in a number of ways according to the objectives of the mission. The configuration will also depend on the availability of LORAN-C and GPS equipment. In spite of this, the functionality of the major components in the system remain constant with each configuration. These include a vehicle mounted component, referred to as the remote unit, and a stationary component, referred to as the monitor unit. Two examples of LORCAL^2 configurations are shown in Figures 4.1 and 4.2. Figure 4.1 shows the configuration which was used

during the winter and summer 1991 field campaigns in the lower St. Lawrence region of Québec [Townsend et al, 1992a]. This configuration, and others similar to it, were used up until November 1991.

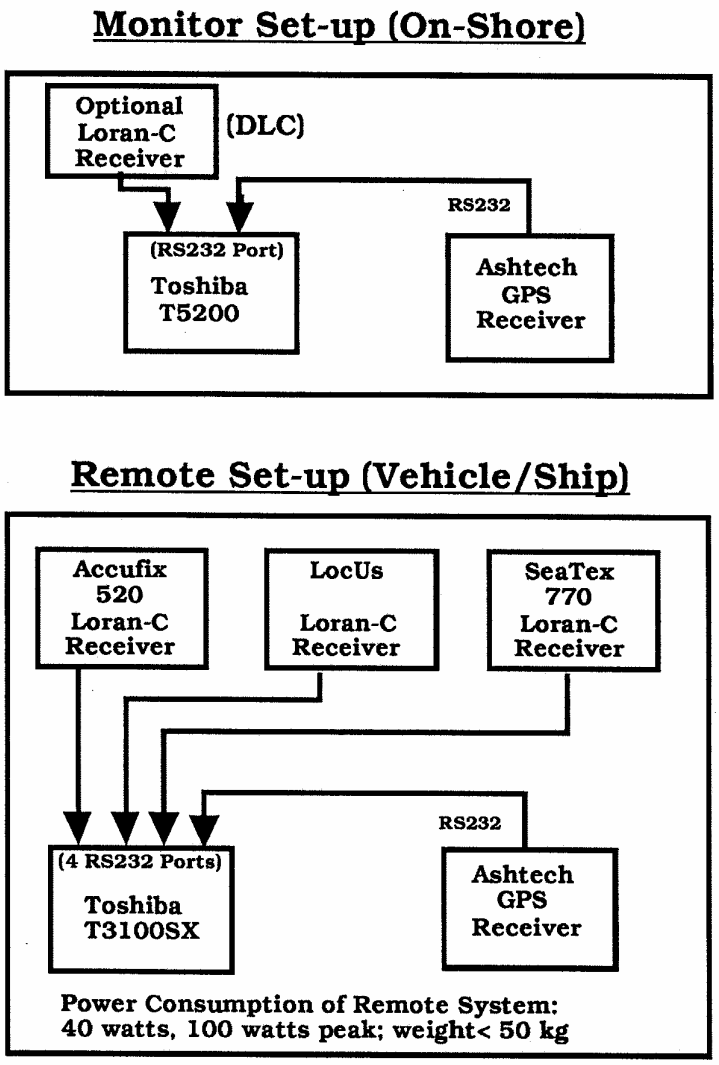

Figure 4.1: LORCAL^2 System Configuration Winter and Summer 1991

Figure 4.2 shows the configuration that was used in May 1992 on a field campaign through the Rocky Mountains of British Columbia [Lachapelle and

Townsend, 1993]. Similar configurations to this were used on all projects after November 1991.

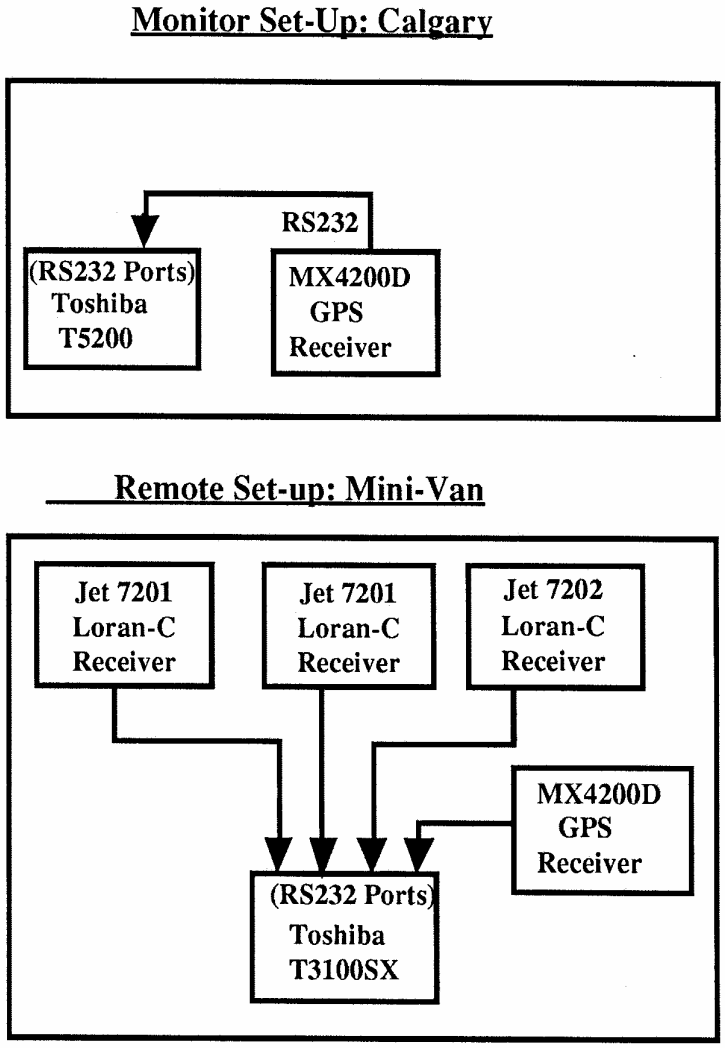

Figure 4.2: LORCAL^2 System Configuration Used May 1992

The remote component of LORCAL^2 consists of one GPS receiver, two to three LORAN-C receivers, and a data logging computer. It could operate with a single LORAN-C receiver, but in the interests of maintaining a high degree of reliability and integrity of the system, it is desirable to have at least two. Both the LORAN-C and GPS receivers must be capable of outputting measurements at a 5 second

rate or faster. This is necessary since a requirement of the system is to collect kinematic data at normal vehicle cruising speeds. The data logging computer must be capable of collecting and storing the data at these high rates. The data volume can be as high 5 megabytes per hour depending on the number of receivers and their output rates. The average data volume is 2 to 3 megabytes per hour. The data logging computer must also be rugged enough to handle the rough field conditions.

The monitor component of LORCAL^2 consists of a GPS receiver situated at a point with known coordinates. The data collected here is used to differentially correct the GPS data collected at the remote unit to produce position coordinates accurate to ≤ 5 m. If the measurement campaign does not require this level of accuracy, one can use the stand alone GPS at the remote unit with an accuracy of 100m, with SA on , or 30 m, with SA off, in which case the monitor component is not required. A LORAN-C receiver can be added to the monitor unit if differential LORAN-C data is required. This function is not often used because, as explained in Section 3.2, as long as abnormal weather anomalies are accounted for, an acceptable accuracy level can be achieved by using standard atmospheric parameters to correct the measurements.

The following describes the various LORAN-C receivers, GPS receivers, and data logging computers used to collect the LORCAL^2 data presented in this thesis.

- Loran-C receivers:

  (i) Accufix 520: This is an analog unit manufactured by Megapulse. It is a proven and sophisticated unit built specially for R&D applications. The single chain unit measures TDs, SNR, FS, and ECD.

(ii) LocUS Pathfinder: This is a digital unit which is a new type of receiver based on a Linear Ensemble Averaging technique claimed to enhance the performance of signal measurements [Post, 1989]. The unit also outputs single chain TDs, SNR, FS, and ECD.

(iii) SeaTex 770: This is an analog receiver which was provided by IML (Institut Maurice-Lamontagne) during the data collection campaign in the Quebec Region. This single chain unit measures TDs. A status indicator provides OK/NOT OK information status on SNR.

(iv) JET 7201: Incorporates combination of digital and analog architecture. It is a multi-chain unit capable of tracking up to eight transmitters from four different chains simultaneously. The unit outputs TOA, SNR, FS, ECD, and atmospheric noise for each transmitter.

(iv) JET 7202: Has the same features as the Jet 7201 but is more compact and lighter weight.

- GPS receivers:

(i) Ashtech LD-XII: This is a 12-channel C/A code unit which outputs raw pseudorange and carrier phase measurements for all satellites in view as well as single point GPS positions which are used in real time for vehicle navigation and data verification.

(ii) Magnavox MX4200D: This is a six-channel unit which outputs raw pseudorange and carrier phase measurements as well as real time positions.

- Data logging computer systems:

  (i) Toshiba T3100SX: This is a DC unit equipped with a 40 MB internal hard disk, a 386SX microprocessor, and multiple RS-232 ports. The unit is used for logging and precise time tagging of the kinematic Loran-C and GPS data at a user selectable rate. It was almost exclusively used at the remote unit because of its light weight, ruggedness, and low power consumption.

  (ii) Toshiba 5200: This is an 386-based AC unit equipped with a 100 MB internal hard disk. It was primarily used at the monitor because of its AC power requirement.

  Both PC units were also used for data validation in the field.

4.3 LORCAL^2 Software Configuration

The software required to drive LORCAL^2 is summarized in the flow chart in Figure 4.3. It is categorized into the following three areas:

(i) Navigation and Data Collection (Real-Time),

(ii) Data Processing and Integrity Checking (Real-Time and Post -Processing), and

(iii) Data Analysis and Result Presentation (Post-Processing).

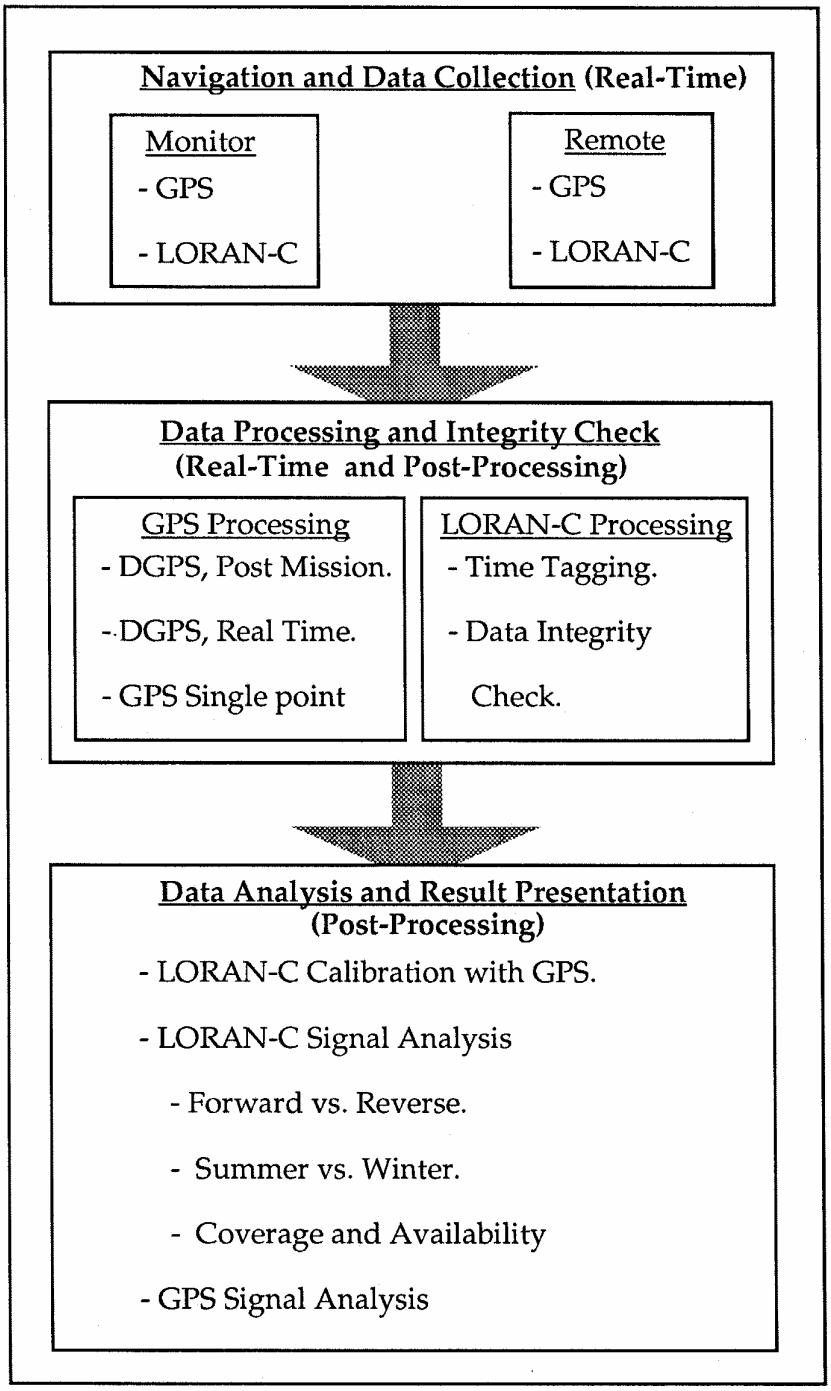

Figure 4.3: LORCAL^2 Software Flow Chart

The data collection software is the most important component of the LORCAL^2 system in terms of function and reliability. It is able to receive, time stamp, and record up to four data streams simultaneously through four RS-232 serial ports. The software accomplishes this by servicing the hardware interrupt lines on each port, thereby, allowing for high data transmission rates and, at the same time, minimizing the data loss associated with sequentially polling of each port.

Time stamping of each LORAN-C measurement is crucial for LORAN-C calibration since the vehicle is in kinematic mode and the best way to compare simultaneous GPS and LORAN-C measurements in post mission is by matching their measurement times.

The LORAN-C measurements are time stamped with the data logging computer system time. The GPS measurements are time stamped with GPS system time. The relationship between the computer system time and GPS system time is obtained by a special task within the data collection software. A one pulse per second (pps) signal is continually sent from the GPS receiver to the computer. The data collection software is triggered by this signal and responds by recording the computer system time along with the corresponding GPS time. The data is used in post mission to convert from the computer system time frame to the GPS time frame.

The data collection software also outputs information to the display screen which allows the operator to monitor the status of each GPS and LORAN-C sensor. The operator can also time tag and record events via the keyboard while in kinematic mode. When a key is struck the software immediately reads the computer

system time and records it along with the character associated with the key that was pressed.

The GPS data processing is necessary to produce the reference trajectory of the remote system platform. This is obtained from one of the following sources:

(i) Post Processed DGPS. It involves post mission processing of the monitor and remote GPS data to produce accurate, differentially corrected GPS positions.

(ii) Real Time DGPS. The monitor GPS data is transmitted to the remote GPS receiver and differentially corrected GPS positions are computed internally by this receiver. These accurate positions are sent to the data logging computer where they are stored for future use.

(iii) SGPS (Single Point GPS). There are two options here: the real time position internally generated by the remote GPS receiver or the position produced from post processed pseudorange data can be used.

Option (i) is the most commonly used because it provides the high level of accuracy required for LORAN-C calibration while not requiring the extra hardware and logistics involved in maintaining a data link between the monitor and remote. Option (ii) was only used in one LORCAL^2 survey located in the Dixon Entrance area off the coast of British Columbia [Lachapelle et al, 1993a]. Option (iii) is always available and acts as a safety net in that the mission can still produce useful results when the monitor station malfunctions and DGPS processing is not possible. This did happened in some instances.

The LORAN-C data processing primarily consists of converting the LORAN-C measurements into the GPS time frame. In doing so, the data is automatically checked for data recording errors and any suspect records are omitted. Single point LORAN-C, and possibly DLC, positions can be computed also.

The analysis and results section of the software flow chart will depend largely on the objectives of the project. Chapters 5 will demonstrate several ways of analysing LORCAL^2 data by reviewing several case studies.

4.4 LORCAL^2 Error Sources

The error sources affecting LORAN-C calibration with LORCAL^2 are as follows:

(i) internal LORAN-C receiver noise, ≤ 10 m,

(ii) dynamic effects, due to receiver motion, ≤ 50 m,

(iii) GPS time synchronization error, ≤ 5 m,

(iv) DGPS position error, 3 - 10 m 2-D RMS (HDOP ≤ 5).

The error due to the internal LORAN-C receiver measuring noise is a function of receiver quality and LORAN-C signal strength. Under normal signal conditions, receivers used in the research presented herein are rated at the 0.01 to 0.02 μs measuring accuracy level with the exception of the SeaTex 770 which is a lower quality receiver.

Since LORAN-C receivers generally do not account for any doppler effects in their signal processing, a receiver mounted on a moving vehicle will suffer some degradation in signal tracking performance. This will generally manifest itself by a drop in SNR and a noisier TD measurement.

The LORCAL^2 data is collected in kinematic mode with the vehicle cruising at speeds of up to 30 m s^{-1}. In order for a valid comparison of GPS and LORAN-C to be made, they must be synchronized in the same time frame. As explained earlier, each data stream within the LORCAL^2 system is time stamped with a high degree of precision by the logging software. This does not, however, remove the data latency internal to the LORAN-C receiver. The latency is caused by a delay between the measurement time and the actual time the measurement is sent to the data logging computer. Most of this effect is calibrated by comparing forward and reverse runs along the same section of road.

The position errors due to GPS are a function of the satellite geometry and distance between the monitor and remote system. This errors were minimized by selecting observation times during good satellite availability periods.

The overall accuracy of the system maybe expressed by the square root of quadratic sum of the above errors which totals 52 m or 0.17μs (1σ). The system was initially tested in a mountainous area north of Vancouver, B.C., in early winter 1991 [Lachapelle et al, 1992a] and the achieved field accuracy was consistent with the above estimate.

CHAPTER 5

LORCAL² CASE STUDIES

5.1 LORAN-C Calibration and Signal Analysis in the Lower St. Lawrence

This case study focuses on a research project carried out by The University of Calgary for the Canadian Hydrographic Service (CHS), Québec Region. The results and analysis presented herein are drawn from the project report and published papers [Townsend et al 1992a, Lachapelle et al 1993b]. The project took place in the Lower St. Lawrence region of Québec as shown in Figure 5.1. The purpose was to study and analyse LORAN-C performance in the area. The measurements were made in 1991.

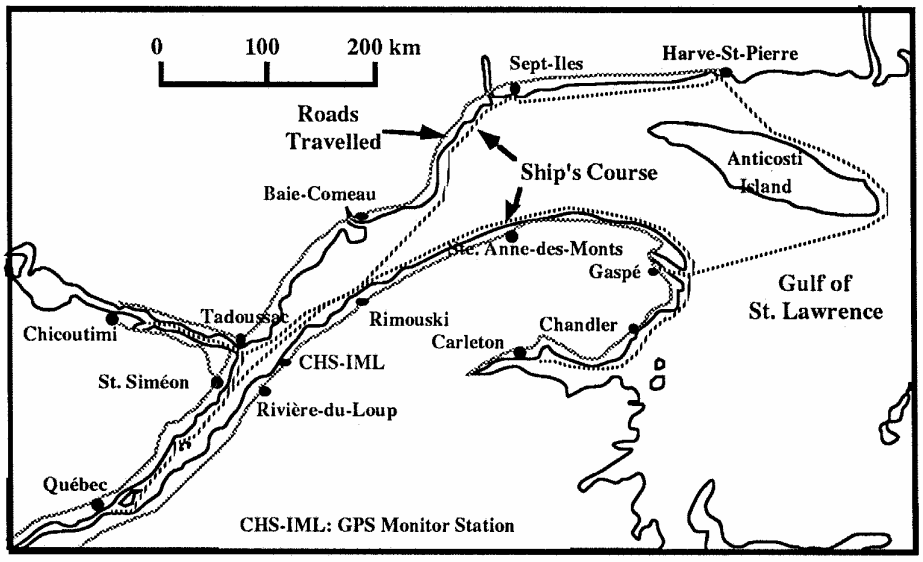

Figure 5.1: Land Roads and Ship Tracks Observed - Winter and Summer 1991

As shown in Figure 5.1, data was collected along several roadways bordering the north and south shores of the St. Lawrence river as well as on the river itself. The

shore data was collected in both the summer and winter seasons. The ship data was collected in the summer only.

The LORAN-C chains operating in the area are shown in Figure 5.2. They are the North East U.S.A. (NEUSA) chain, GRI 9960, the East Coast Canada (ECC) chain, GRI 5930, and the Labradour Sea chain, GRI 7930.

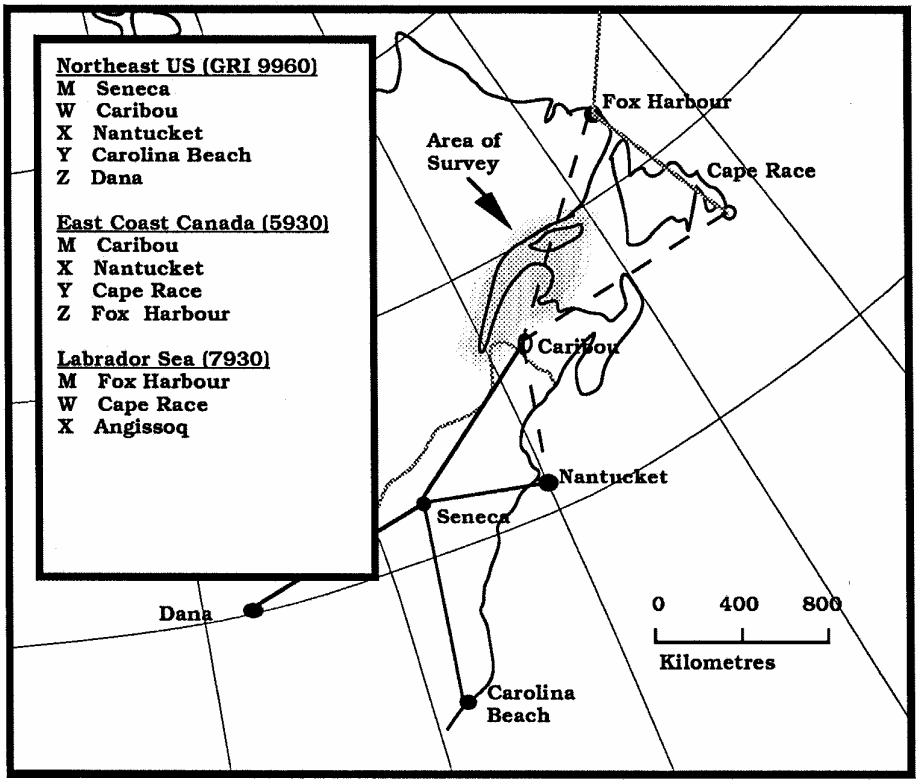

Figure 5.2: Loran-C Chains available in the Lower St. Lawrence Area

The following sub-sections investigate various aspects of LORAN-C performance in the area.

5.1.1 Field Strength , Atmospheric Noise, and SNR Analysis

Presented in this section is an analysis of the predicted FS (Field Strength) and Atmospheric Noise (N_{atm}) for the region shown in Figure 5.1. The predicted results will be used for analysing the measured FS and N_{atm} values in the next section. Both quantities are given in $\mu V\ m^{-1}$ or in dB referred to $1\mu V\ m^{-1}$. Conversion from $\mu V\ m^{-1}$ to dB is accomplished by using the following formula:

$$dB = 20 \log X$$

where X is either FS or N_{atm} in $\mu V\ m^{-1}$.

The FS, at 100 kHz, is mainly a function of transmitter power and conductivity along the propagation path. If one assumes that the conductivity is known and constant along the propagation path, FS can be precisely calculated using finite formulas [e.g., Johler et al, 1956; CCIR, 1988b]. These formulae have been used to generate graphs giving FS as a function of distance for a nominal value of radiated power (e.g., 1 kW) [e.g., Rohan, 1991]. FS for any other radiated power P is then given by

$$FS(\mu v\ m^{-1})_P = FS(\mu v\ m^{-1})_{1\ kW}\ [P(kW)]^{-1/2}$$

or

$$FS(dB)_P = FS(dB)_{1\ kW} + 20 \log \{[P(kW)]^{-1/2}\}$$

The above technique was used to derive Figure 2.12 where the calculated FS is plotted as a function of the length of the propagation path for various ground conductivities and for a radiated power of 400 kW. The difference between the good conductor, for example, seawater at 5 S m^{-1}, and a very poor conducting soil at 0.001 S m^{-1}, grows as a function of the distance from the transmitter. At

1,000 km, the difference is nearly 10 dB. When the conductivity varies along the path, FS can be calculated using Millington's method [Samaddar, 1980]. Since the exact conductivity along the propagation path is not exactly known, especially in the case of overland paths, an average conductivity is usually used to estimate FS. This was done in the present case. The best a priori value estimated for the area under consideration is 0.001 S m^{-1}, according to the Morgan conductivity survey performed in the 1960s [Hamilton, 1987].

The atmospheric noise is not measured directly by a Loran-C receiver but derived using the following equation:

$$N_{atm_{meas}} = FS_{meas} - SNR_{meas}.$$

The atmospheric noise N_{atm} is a function of thunderstorm activities around the world and has been estimated by CCIR [1988a] for the 1 MHz frequency range using data collected at various locations. The estimated values are a function of location, season, and time of day. CCIR [1988a] gives world maps showing estimated noise in dB for each period of 4 hours intervals for each season. This allows one to take the diurnal and seasonal effects into account. The rms noise field strength at a given frequency is calulated by

$$N_{atm}(dB) = F_a - 95.5 + 20 \log f_{MHz} + 10 \log b$$

where F_a is the rms noise value extracted from the CCIR maps (at 1 MHz), f_{MHz} is the frequency correction factor for the LORAN-C frequency (0.1 MHz) from additional maps given in CCIR [1988a], and b is the LORAN-C bandwitdth in Hz (i.e., 20,000 Hz). The above formula was used to calculate N_{atm} for the area under consideration and the results are shown in Table 5.1. The differences

between summer and winter range from 2 to 15 dB, the noise being higher in summer. An atmospheric noise value of 61 dB for the areas covered by the 9960 and 5930 Chains has recently been predicted by the U.S. Department of Transportation [U.S. DoT, 1992] which is considerably higher than the values given in Table 5.1. This value was obtained by assuming the worst case, which occurs during late evenings in summer. In order to obtain such a high value from the CCIR maps, one would select the largest N_{atm} corresponding to summer evenings in the area and add another 10 to 20 dB as a safety factor. Both the constant 61 dB value and the values given in Table 5.1 were tested. An analysis of both summer and winter data showed no significant diurnal or seasonal variations. Moreover, the measured atmospheric noise agreed with the predicted constant value of 61 dB within a few dBs.

Table 5.1: Predicted Atmospheric Noise in the Lower St.Lawrence Area *

Time Interval	Winter	Summer
0000 - 0400h	37.5 dB	49.5 dB
0400 - 0800	32.5	35.5
0800 - 1200	22.5	32.5
1200 - 1600	22.5	37.5
1600 - 2000	29.5	37.5
2000 - 2400	35.5	47.5

* Predictions based on CCIR data [CCIR, 1988a]

As an example, measured and predicted FS, SNR and N_{atm} values obtained in winter 1991 are compared at representative points in Tables 5.2.

Table 5.2: Predicted Versus Observed FS and SNR (Winter 1991)

Location/ Transmitter	Date	Time	M* FS	P* FS	Δ* FS	N_{atm}	M SNR	P SNR	Δ SNR	P Δ SNR (Nc)
9960M										
Beauport	Mar 19	06h	64	63	1	32	5	32	-27	2
Rivière-du-Loup	Mar 19	21h	59	57	2	34	0	25	-25	3
Rimouski	Mar 21	23h	56	53	3	36	-4	20	-24	2
Baie-Comeau	Mar 20	08h	45	51	-7	27	0	18	-18	16
Sept-Iles	Mar 20	17h	46	45	1	28	-10	17	-27	5
Gaspé	Mar 17	11h	38	44	-6	23	-15	15	-31	8
9960W										
Beauport	Mar 19	06h	77	83	-6	32	7	45	-38	-9
Riviere-du-Loup	Mar 19	21h	82	88	-6	34	7	48	-41	-14
Rimouski	Mar 21	23h	78	86	-8	36	7	42	-35	-10
Baie Comeau	Mar 20	08h	72	82	-10	27	7	45	-38	-4
Sept-Iles	Mar 20	17h	72	74	-2	28	7	44	-37	-4
Gaspé	Mar 17	11h	66	77	-11	23	5	44	-39	0
9960X										
Beauport	Mar 19	06h	60	61	-1	32	4	28	-24	5
Riviere-du-Loup	Mar 19	21h	60	56	4	34	2	26	-24	3
Rimouski	Mar 21	23h	53	53	0	36	-6	17	-23	2
Baie Comeau	Mar 20	08h	47	51	-4	27	2	20	-18	16
Gaspé	Mar 17	11h	50	49	1	23	-5	28	-33	6

* - M = Measured, P = Predicted, Δ = difference.
- All FS and SNR values in dB (referred to 1 μvm^{-1})
- Pred. SNR = Measured FS - Predicted atmospheric noise
- ΔSNR_{Nc} is based on the use of a predicted constant atmospheric noise value of 61 dB [U.S. DoT, 1992].

Table 5.2 (con't): Predicted Versus Observed FS and SNR (Winter 1991)

Location/ Transmitter	Date	Time	M* FS	P* FS	Δ* FS	N_{atm}	M SNR	P SNR	Δ SNR	PΔ SNR (Nc)
5930M										
Beauport	Mar 19	06h	78	83	-5	32	23	46	-23	6
Riviere-du-Loup	Mar 19	21h	84	88	-4	34	19	51	-32	-5
Rimouski	Mar 21	23h	86	86	0	36	20	50	-31	-6
Baie Comeau	Mar 20	08h	78	82	-4	27	22	51	-29	5
Sept-Iles	Mar 20	17h	76	74	2	28	16	47	-31	2
Gaspé	Mar 17	11h	76	77	-1	23	19	53	-35	4
5930X										
Beauport	Mar 19	06h	62	61	1	32	10	30	-20	9
Riviere-du-Loup	Mar 19	21h	65	56	9	34	1	31	-30	-3
Rimouski	Mar 21	23h	55	53	2	36	-7	19	-26	-1
Baie Comeau	Mar 20	08h	53	51	2	27	0	26	-26	8
Sept-Iles	Mar 20	17h	53	46	7	28	-6	25	-31	2
Gaspé	Mar 17	11h	59	49	10	23	7	37	-30	9
5930Y										
Beauport	Mar 19	06h	44	38	6	32	-7	12	-19	10
Riviere-du-Loup	Mar 19	21h	54	43	11	34	-9	20	-29	-2
Rimouski	Mar 21	23h	55	46	9	36	-7	19	-26	-1
Baie Comeau	Mar 20	08h	50	46	4	27	-2	23	-25	9
Sept-Iles	Mar 20	17h	53	49	4	28	-6	25	-31	2
Gaspé	Mar 17	11h	62	56	6	23	6	40	-34	5
5930Z										
Beauport	Mar 19	06h	44	41	3	32	-6	12	-18	11
Riviere-du-Loup	Mar 19	21h	40	46	-6	34	-23	6	-29	-2
Rimouski	Mar 21	23h	48	51	-3	36	-15	12	-27	-2
Baie Comeau	Mar 20	08h	35	52	-17	27	-16	8	-24	10
Sept-Iles	Mar 20	17h	43	58	-15	28	-16	15	-31	2
Gaspé	Mar 17	11h	55	59	-4	23	-1	33	-34	5

The predicted SNR was calculated as follows:

$$SNR = FS_{meas} - N_{atm_{pred}}$$

The delta-SNR's (ΔSNR's) were obtained using the N_{atm} values of Table 5.1, while the ΔSNR_{N_c}'s were obtained using a constant N_{atm} of 61 dB. The differences between measured and predicted FS are generally within a few dBs for overland paths. This indicates that the conductivity of 0.001 S m^{-1} selected to predicted FS values is realistic. For mixed land-water paths, the best agreement (not shown in Table 5.2) was obtained using Millington's method. The recovery effect was noticable at many locations. The differences between measured and predicted SNR values are much smaller when a constant value of 61 dB is used. This value, used by the U.S. DoT [1992], is, therefore, more realistic than the values predicted using the CCIR data. Similar results were obtained for the summer data.

Specific comments on the FS and SNR values for each chain are as follows:

<u>East Coast Canada Chain (5930)</u>

- The measured field strengths are generally within 5 to 10 dB of the predicted values, except for the signals transmitted from Fox Harbor. This sugguests that the 0.001 S m^{-1} conductivity value used for the surrounding land is realistic. In the case of 5930X and Y, the measured field strengths are generally stronger than the predicted ones. This is due to the sea path over parts of the transmission as can be seen from Figure 5.2. The use of Millington's method to predict FS based on mixed land/sea path would have likely resulted in a better agreement.

- The measured FS values from 5930Z (Fox Harbour) are much lower than the predicted values between Baie-Comeau and Havre-St-Pierre, on the North Shore, than in any other area. This is because the propagation path is completely overland between Fox Harbour and that part of the North Shore. The conductivity of that rocky part of the Canadian shield is known to be extremely low and the value of 0.001 S m^{-1} used in this particular case is too optimistic. At other sites, further away from Fox Harbour than the Baie-Comeau Havre-St-Pierre area, the difference is not so large due to propagation over water. This is a classic case of a recovery effect which could be predicted quite accurately using Millington's method. Due to the above, reception of 5930Z was marginal (< -10 dB) except around the Gaspé Peninsula where the recovery effect due to sea water between Anticosti Island and the Gaspé Peninsula was sufficient to bring the SNR above the -10dB threshold.

- The use of a constant value of 61dB for the atmospheric noise N_{atm} resulted in a much better agreement between predicted and measured SNR values. Although, the differences on most transmitters tends to be systematically positive, indicating that the atmospheric noise may be below the value of 61dB by a few dB in that part of the chain coverage due to its more northern latitude. Predicted atmospheric noise drops considerably as latitude increases [CCIR, 1988a]. It should however be noted that the measured SNR is also a function of the receiver used. The SNR measured with the LocUS Pathfinder receiver was generally some 5 to 10 dB higher than that measured with the Accufix 520.

Northeast U.S. Chain (9960):

- The SNR was generally ≥ -10 dB for M (Seneca), W (Caribou) and X (Nantucket). Reception of Y (Carolina Beach) and Z (Dana) was marginal due to the relatively large distances from these transmitters over land propagation paths. As the SNR values on both Y and Z were consistently ≤10dB, these measurements are not listed.

Labrador Sea Chain (GRI 7930):

- Only M (Fox harbour) and W(Cape Race) could be observed around the Gaspesia Peninsula. No direct measure of the SNR is available on the SeaTex receiver used. Instead, a good/poor signal reception indicator is used. The results obtained for M and W are generally consistent with those obtained on 5930Z and 5930Y since these are the same transmitters. The use of this single TD measurement from the Labrador Sea Chain in the Gaspesia Peninsula would require the use of a multi-chain receiver and this would result in only marginal improvements since there would be no gain in geometry.

5.1.2 Winter versus Summer DTD Road Measurements

The LORAN-C TD distortion DTD, is defined herein as

$$DTD = TD_{LORAN\text{-}C} - TD_{GPS}$$

where $TD_{LORAN\text{-}C}$ is the measured Time Difference, and TD_{GPS} is the corresponding Time Difference derived using DGPS positions

The winter and summer road measurements were made primarily to assess the seasonal effects on the DTDs. The differences between winter and summer

averages were then calculated. The statistics of the differences are shown in Tables 5.3 and 5.4. The actual DTD's are given in [Lachapelle et al, 1993].

Table 5.3: Comparison of Winter and Summer Road DTDs Measured With LocUS Pathfinder On Chain 5930

Data Set		[Winter - Summer] Statistics*		
		5930X	5930Y	5930Z
North Shore	Samples	118	91	15
	Mean	-0.17	-0.17	-0.20
	RMS	0.20	0.24	0.30
	St. dev.	0.11	0.17	0.21
South Shore	Samples	198	134	29
	Mean	-0.19	-0.24	-0.22
	RMS	0.21	0.27	0.28
	St. dev.	0.09	0.12	0.17

* All means, rms and standard deviations are in μs.

The relatively low number of samples is due to the commonality requirement between the averaged data points. However, because each comparison is actually derived from a large number of individual measurements, the statistics are significant. The mean differences reach -0.24 μs, which is equivalent to a range difference of 72 m. Seasonal differences are usually due to the combination of two seasonal effects, namely variations in the primary and secondary phase lags. In order to test whether seasonal variations in the primary phase lag could account for the above difference, the effect of the primary phase lag on TD measurements made on the East Coast Canada Chain was calculated using two

values for refractivity, namely 310 and 330. These values correspond to extreme winter and summer conditions, respectively, in the area of the survey [Segal and Barrington, 1977]. The average difference between the two sets of TDs generated with the above two refractivity coefficients was 0.04μs, well below the average value of 0.20μs implied by the results shown in Table 5.3. The seasonal variations are, therefore, likely caused by changes in conductivity between winter and summer. Nevertheless, the variations do not appear to be sufficiently large to justify the use of seasonally adjusted LORAN-C grid corrections for marine navigation in the area.

Table 5.4: Comparison of Winter and Summer Road DTDs Measured With Accufix 520 On Chain 9960

Data Set		[Winter - Summer] Statistics*	
		9960W	9960X
North Shore	Samples	25	29
	Mean	0.10	-0.09
	RMS	0.22	0.14
	St. dev.	0.19	0.12
South Shore	Samples	127	122
	Mean	0.01	-0.17
	RMS	0.14	0.21
	St. dev.	0.14	0.14

* All means, rms and standard deviations are in μs.

5.1.3 Across-Chain (5930 Versus 9960) TD Comparison

The 5930X TD is given by:

$$TD(5930X) = TOA(5930M\text{-}Caribou) - [TOA(5930X\text{-}Nantucket) - 13131.88\mu s]$$

where 13131.88μs is the fixed ED of 5930X [CCG, 1990; USNO, 1992]. The 9960X and W TDs are given by:

$$TD(9960X) = TOA(9960M\text{-}Seneca) - [TOA(9960X\text{-}Nantucket) - 26969.93\mu s]$$
$$TD(9960W) = TOA(9960M\text{-}Seneca) - [TOA(9960W\text{-}Caribou) - 13797.20\mu s]$$

If all transmitters in both chains were transmitting on precisely the same time scale, we would expect the following relationship to hold, within the accuracy of the measurements:

$$[TD(9960X) - TD(9960W)] - TD(5930X) = 0$$

The above differences are shown in Figures 5.3 and 5.4 for some of the measurements taken along roads bordering the South Shore and some measurements taken on the ship, respectively. The road measurements taken in forward and reverse directions both during winter and summer 1991 were averaged. The ship measurements were taken during summer 1991. An average difference of 0.46 to 0.48μs is present in both cases. The standard deviation of one difference varies between 0.07 and 0.11μs. The difference of nearly 0.5μs, which corresponds to a range difference of 150 m, is due to time scale variations between the transmitters such as biases in the emission delays. For instance, the area monitors control the TDs in their respective areas to ensure a high degree of position repeatability. The area monitors for 5930X, 9960X and 9960W are

located in Montague, PEI, Sandy Hook, NJ, and Cape Elizabeth, ME, respectively. Initial differential position errors between the monitors and the transmitters, for instance, could cause the above constant difference of 0.5μs.

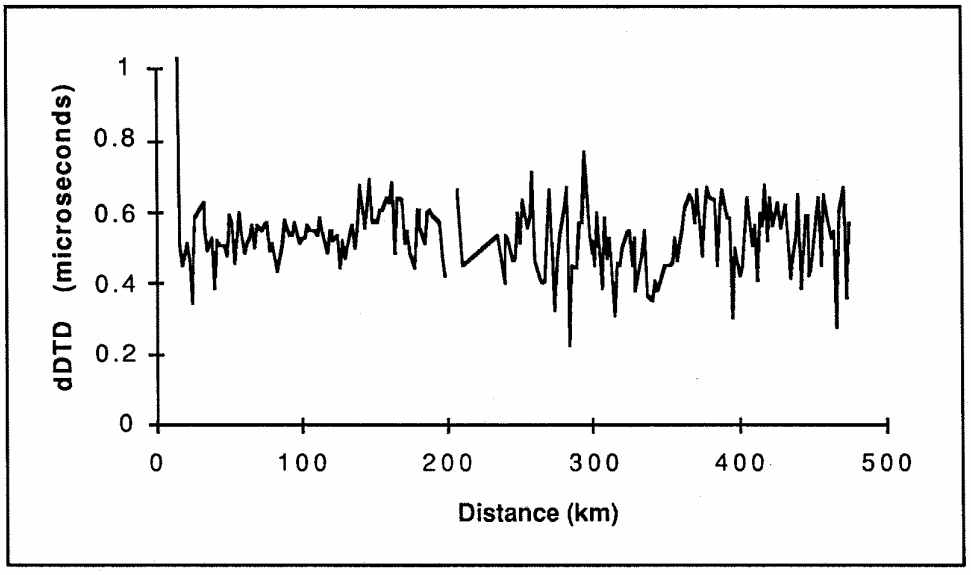

Figure 5.3: [TD(9960X) - TD(9960W)] - TD(5930X), South Shore Road Measurements

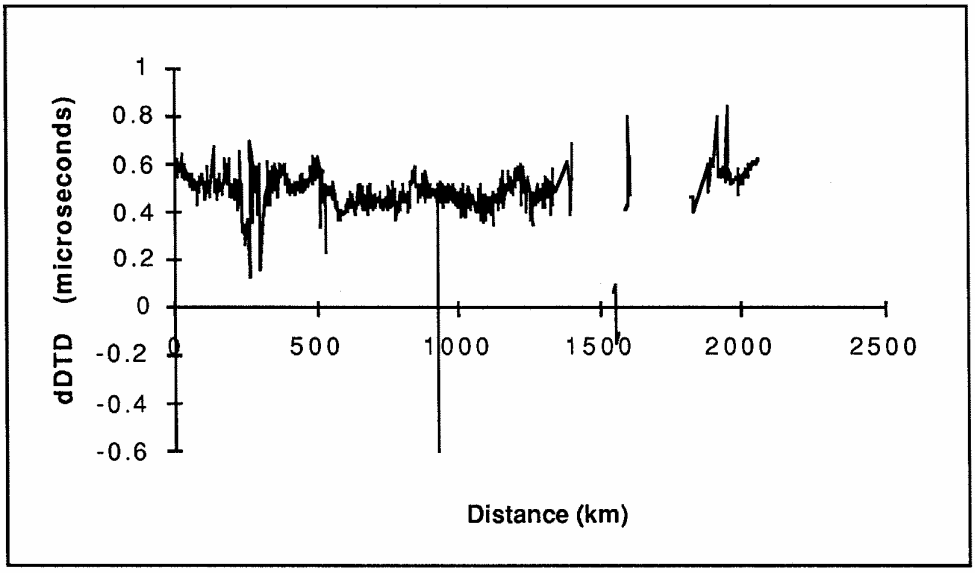

Figure 5.4: [TD(9960X) - TD(9960W)] - TD(5930X), Ship Measurements

The difference would not have any effect on the use of a multi-chain receiver which would use calibrated TDs from both chains simultaneously, however, since each TD is calibrated separately herein.

5.1.4 Modelled Versus GPS-Derived DTDs

In order to analyse the differences between modelled and GPS-derived DTDs, a series of numerical tests summarized in Table 5.5 and 5.6 were conducted. Table 5.5 summarizes the results obtained with the road data while Table 5.6 summarizes the results obtained with the ship data.

The primary phase lag (PF) was modelled using a constant refractivity of 320 which corresponds to a refractive index of 1.000320. The combined effect of the secondary (SF) and additional secondary (ASF) phase lags was modelled using successive values of 5 S m^{-1}, 0.005 S m^{-1} and 0.001 S m^{-1} for conductivity. The highest value corresponds to a propagation path completely over sea water. The lowest value corresponds to the estimated soil conductivity in the area covered by the two chains [Hamilton, 1987].

The mean DTDs when no phase factor is applied to the Loran-C measurements reaches -4.6μs. The application of PF, SF and ASF corrections with a conductivity of 5 S m^{-1} results in the best agreement, both in terms of mean and rms values, in the case of the East Coast Canada Chain (5930), both for the road and ship data. The use of a conductivity value of 0.001 S m^{-1}, however, results in the best agreement in the case of the Northeast U.S. Chain. This is because of the effect of the sea water on most propagation paths from the 5930 transmitters to the survey area, as can be seen in Figure 5.2. The use of Millington-Plessey's technique to

model the effect of SF and ASF along the mixed path would more likely improve the agreement between GPS-derived and modelled DTDs significantly.

Table 5.5: Modelled Versus GPS-Derived DTDs*, Road Measurements

Data Set		Transmitters				
		5930X	5930Y	5930Z	9960W	9960X
North Shore	Mean	2.33	3.57	3.22	-4.59	-1.96
no PF applied	RMS	2.35	3.74	3.32	4.68	2.05
no SF+ASF applied	St. dev.	0.32	1.09	0.82	0.88	0.59
North Shore	Mean	1.68	2.72	2.63	-3.92	-1.90
N = 320	RMS	1.70	2.86	2.71	4.00	1.99
no SF+ASF applied	St. dev.	0.27	0.89	0.64	0.79	0.58
North Shore	Mean	0.52	1.16	1.60	-2.78	-1.77
N = 320	RMS	0.56	1.30	1.70	2.85	1.85
$s = 5\ S\ m^{-1}$	St. dev.	0.22	0.59	0.58	0.62	0.54
North Shore	Mean	-1.16	-0.85	0.02	-0.91	-1.72
N = 320	RMS	1.18	1.00	0.93	1.04	1.82
$s = 0.005\ S\ m^{-1}$	St. dev.	0.21	0.53	0.93	0.51	0.58
North Shore	Mean	-1.77	-1.71	-0.46	-0.20	-1.57
N = 320	RMS	1.78	1.85	1.40	0.45	1.65
$s = 0.001\ S\ m^{-1}$	St. dev.	0.20	0.71	1.32	0.41	0.50
South Shore	Mean	1.90	3.03	2.55	-3.56	-1.02
no PF applied	RMS	1.98	3.46	2.91	3.66	1.16
no SF+ASF applied	St. dev.	0.53	1.67	1.40	0.86	0.55

* All means, rms and standard deviations are in μs.

Table 5.5 (con't): Modelled Versus GPS-Derived DTDs*, Road Measurements

Data Set		Transmitters				
		5930X	5930Y	5930Z	9960W	9960X
South Shore	Mean	1.28	2.14	1.94	-2.87	-0.93
N = 320	RMS	1.37	2.59	2.29	2.96	1.07
no SF+ASF applied	St. dev.	0.50	1.46	1.22	0.74	0.52
South Shore	Mean	0.21	0.56	0.89	-1.72	-0.75
N = 320	RMS	0.53	1.23	1.29	1.79	0.89
s = 5 S m^{-1}	St. dev.	0.49	1.09	0.93	0.51	0.48
South Shore	Mean	-1.57	-1.62	-0.89	0.25	-0.60
N = 320	RMS	1.62	1.76	1.12	0.55	0.74
s = 0.005 S m^{-1}	St. dev.	0.40	0.71	0.68	0.49	0.43
South Shore	Mean	-2.17	-2.39	-1.37	0.99	-0.46
N = 320	RMS	2.20	2.44	1.48	1.09	0.62
s = 0.001 S m^{-1}	St. dev.	0.38	0.48	0.55	0.45	0.42

* All means, rms and standard deviations are in μs

The residual DTDs constitute the accuracy gain obtained by using GPS to calibrate the LORAN-C TDs. The mean and rms values of these residuals exceed 1μs in many cases, even when using the conductivity which minimizes these values. The effect of these residuals on LORAN-C positions is a function of the transmitters used and their geometry. The effects, in terms of latitude (ΔLAT) and longitude (ΔLON) errors for each possible combination of transmitters, are given for a selected point near Rimouski in Table 5.7. Two conductivity values were used, namely 0.001 S m^{-1} and 5 S m^{-1}. The coordinate errors are very sensitive to the conductivity and the geometry of the transmitters used, but are

generally less than 1,000 m when the HDOP (Horizontal Dilution of Precision) is better (lower) than 2.0.

Table 5.6: Modelled Versus GPS-Derived DTDs*, Ship Measurements

Data Set		Transmitters				
		5930X	5930Y	5930Z	9960W	9960X
	Mean	1.95	3.01	2.94	-4.23	-1.50
no PF applied	RMS	2.05	3.38	3.36	4.34	1.78
no SF+ASF applied	St. dev.	0.63	1.52	1.64	0.96	0.96
	Mean	1.32	2.22	2.31	-3.52	-1.40
N = 320	RMS	1.46	2.54	2.68	3.62	1.67
no SF+ASF applied	St. dev.	0.61	1.25	1.34	0.87	0.91
	Mean	0.24	0.80	1.28	-2.26	-1.19
N = 320	RMS	0.67	1.12	1.52	2.37	1.45
s = 5 S m^{-1}	St. dev.	0.62	0.79	0.82	0.72	0.83
	Mean	-1.43	-1.16	-0.35	-0.35	-1.02
N = 320	RMS	1.51	1.32	0.74	0.77	1.27
s = 0.005 S m^{-1}	St. dev.	0.48	0.64	0.65	0.69	0.76
	Mean	-1.94	-1.80	-0.91	0.33	-0.89
N = 320	RMS	1.99	1.99	1.31	0.78	1.16
s = 0.001 S m^{-1}	St. dev.	0.42	0.85	0.94	0.70	0.75

* All means, rms and standard deviations are in μs.

Table 5.7: Effect of Residual GPS-Derived Loran-C TD Distortions (DTDs) On Position Fixes

Location: Rimouski, Latitude = 48-28-37, Longitude = -68-30-57

The following are the propagation parameters and corresponding DTDs used for the position computations:

PF = 320 ppm, Conductivity = 0.001 S m^{-1}

DTD(9960W) = 2.15 μs DTD(9960X) = 0.06 μs

DTD(5930X) = -2.55 μs DTD(5930Y) = -3.24 μs DTD(5930Z) = -2.79 μs

PF = 320 ppm, Conductivity = 5 S m^{-1}

DTD(9960W) = -0.83 μs DTD(9960X) = -0.28 μs

DTD(5930X) = 0.10 μs DTD(5930Y) = 0.53 μs DTD(5930Z) = 0.49 μs

0.001 S m^{-1}		5 S m^{-1}					
ΔLat (m)	ΔLng (m)	ΔLat (m)	ΔLng (m)	HDOP	Lat DOP	Lng DOP	Transmitters Used
-2666	-1473	503	412	8.85	8.26	3.18	9960W 9960X
-3181	-1677	-29	199	5.34	5.02	1.82	9960W 9960X 5930X
1069	-59	-264	119	1.24	1	0.73	9960W 9960X 5930Y
646	-230	-164	159	1.03	0.66	0.78	9960W 9960X 5930Z
1085	-203	-264	117	1.22	1	0.71	9960W 9960X 5930X 5930Y
803	-236	-189	126	0.93	0.61	0.7	9960W 9960X 5930X 5930Y 5930Z
1071	-687	-107	-23	2.37	1.23	2.02	5930X 5930Y 5930Z
2808	-2077	-250	91	3.66	2.5	2.67	5930X 5930Y
1419	-2012	-137	86	2.91	1.3	2.6	5930X 5930Z
51	1205	-24	-178	3.58	1.78	3.1	5930Y 5930Z

5.2 Coverage Validation of the NOCUS LORAN-C Chain on the Canadian Prairies

The Loran-C **N**Orth Central **U.S.** (**NOCUS**) Chain has been fully operational since August 1991. Its optimistic and pessimistic coverages in Western Canada, as estimated previously, are shown in Figure 5.5 [Lachapelle et al 1992b]. These estimated coverages were obtained by the U.S. Coast Guard using successively average and worst case atmospheric noise, as calculated at 100 kHz using CCIR data [CCIR, 1988a] and standard noise calculation procedures [e.g., Rohan, 1991]. Seasonal atmospheric noise variations in Western Canada reach about 12 dB, with a minimum in winter and maximum in summer, as expected.

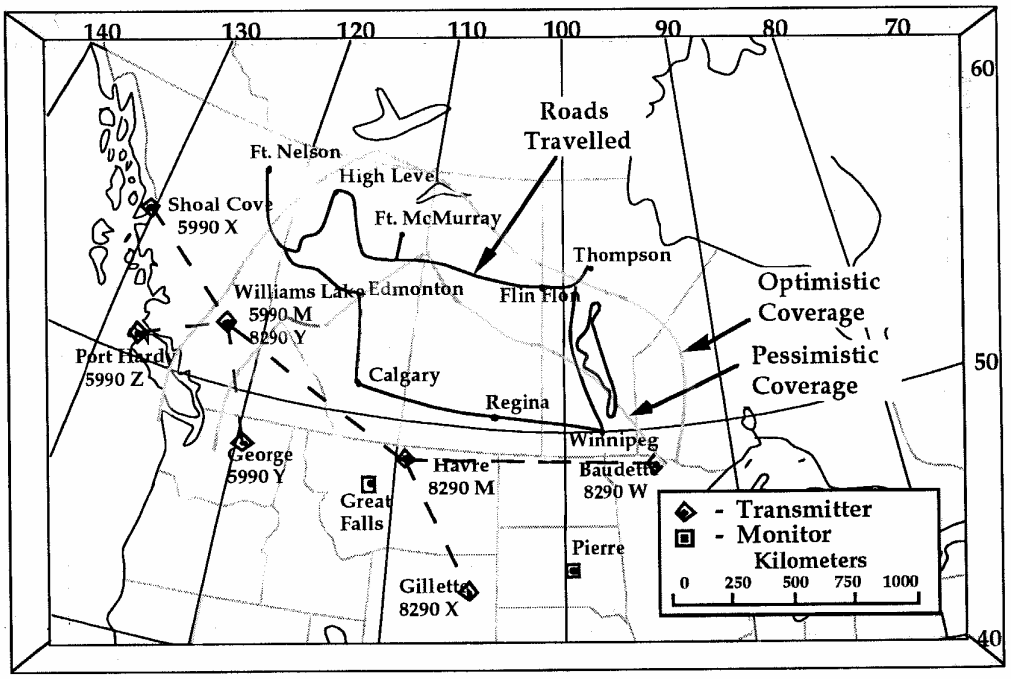

Figure 5.5: A Priori Oprimistic and Pessimistic Northern Extent of NOCUS along with the Route Travelled

The average atmospheric noise in Canada is shown in Figure 2.10. Average conductivity values derived from the 1968 Westinghouse conductivity map (Morgan's) were used. The optimistic coverage extents some 200 to 300 km farther north than the pessimistic coverage and more than doubles the coverage area of NOCUS in Western Canada. A more precise estimation of the actual coverage, based on field measurement is, therefore, important.

Most of the expected NOCUS coverage area in Western Canada consists of flat prairies with ground conductivities of the order of 0.01 S m^{-1}. The western part of the coverage, however, includes an area located in the Canadian Rockies, where the topography is steep and the conductivity is of the order of 0.003 S m^{-1}.

LORAN-C field measurements were conducted during the period 10-19 December 1991 using LORCAL^2 mounted in a mini-van. Most of the measurements were made between 8:00 and 16:00, local time, with a GPS HDOP < 10. Approximately measurements were taken along 5,000 km of road, as shown in Figure 5.5. No measurements were made in the mountainous part of the expected coverage area due to winter road conditions in December. The roads followed were generally the most northerly roads available at that time of the year. The most important localities encountered are indicated on the map, in addition to larger cities located on the Prairies.

The overall characteristics of the signals are summarized in Table 5.8. For each road section shown in Figure 5.5, the range of the SNR, FS, and ECD are given. When the SNR was < -10 dB, no data is reported. When the signals are available, the field strength ranges between 55 and 75 dB. The SNR varies between -10 dB

and 20 dB. The ECD varies between -2 and 4 μs. No data along the Dixonville - High Level road segment could be collected due to the presence of PLC's.

Table 5.8: SNR, FS and ECD -- NOCUS Transmitters

Section of Road	8290 - M			8290 - W			8290 - X			8290 - Y		
	SNR	FS	ECD	SNR	FS	ECD	SNR	FS	ECD	SNR	FS	ECD
Fort St. John to Fort Nelson	15 ↔ 20	60 ↔ 70	1 ↔ 2	--	--	--	--	--	--	15 ↔ 20	65 ↔ 75	1 ↔ 2
Spirit River to Dixonville	14 ↔ 18	65 ↔ 75	1 ↔ 2	0 ↔ 5	50 ↔ 60	0 ↔ 3	0 ↔ 5	50 ↔ 60	2 ↔ 2	14 ↔ 18	70 ↔ 75	0 ↔ 2
*Dixonville to High Level	--	--	--	--	--	--	--	--	--	--	--	--
High Level to Red Earth	10 ↔ 20	65 ↔ 70	0 ↔ 3	-5 ↔ 5	50 ↔ 60	-4 ↔ 4	-5 ↔ 5	50 ↔ 60	0 ↔ 3	10 ↔ 20	60 ↔ 70	-1 ↔ 1
Red Earth to Athabasca	10 ↔ 20	70 ↔ 75	1 ↔ 3	-5 ↔ 5	55 ↔ 65	0 ↔ 3	0 ↔ 5	50 ↔ 60	1 ↔ 3	10 ↔ 20	60 ↔ 70	-1 ↔ 2
Athabasca to Fort McMurray	5 ↔ 20	70 ↔ 75	2 ↔ 4	-5 ↔ 0	55 ↔ 65	2 ↔ 4	-5 ↔ 5	55 ↔ 65	1 ↔ 4	5 ↔ 20	60 ↔ 70	1 ↔ 3
Fort McMurray to Lac La Biche	10 ↔ 20	70 ↔ 75	1 ↔ 3	0 ↔ 10	55 ↔ 65	1 ↔ 4	0 ↔ 10	55 ↔ 65	1 ↔ 4	10 ↔ 20	65 ↔ 75	-1 ↔ 2
Lac La Biche to Meadow Lake	15 ↔ 20	70 ↔ 75	2 ↔ 3	0 ↔ 10	60 ↔ 70	1 ↔ 3	0 ↔ 10	55 ↔ 65	1 ↔ 4	15 ↔ 20	55 ↔ 65	-2 ↔ 2
Meadow Lake to Flin Flon	10 ↔ 20	70 ↔ 75	1 ↔ 3	5 ↔ 15	70 ↔ 75	0 ↔ 3	0 ↔ 10	65 ↔ 75	-2 ↔ 4	--	--	--
Flin Flon to Thompson	10 ↔ 20	65 ↔ 75	1 ↔ 3	5 ↔ 15	60 ↔ 75	0 ↔ 3	5 ↔ 15	60 ↔ 70	-2 ↔ 2	--	--	--

The Fort St. John - Fort Nelson area is outside the NOCUS coverage since only two transmitters, namely M and Y, can be received in that area. However, the use of the JET 7201 multi-chain receiver provided Loran-C positions by combining NOCUS and WCC data together.

The continuous northern extent of NOCUS which can be estimated at this time using the above data is shown in Figure 5.6, together with the SNRs measured at selected northerly sites. The SNRs at these points are ≥ -3 dB. Since a minimum of -10 dB is sufficient for land applications, this would suggest that the coverage may extent another 100 to 200 km beyond the limit shown here. However, the measurements were made in winter, between 8:00 and 16:00, when both seasonal and diurnal atmospheric noise values are normally at a minimum. An adjustment to account for the higher diurnal noise under summer conditions is

not as trivial as it may seem. A straight use of CCIR predicted atmospheric noise would require a correction to the SNR values shown in Figure 5.6 in excess of -10 dB, in which case the coverage shown in the figure could be interpreted as optimistic. However, Loran-C SNR analysis over different seasons in the St. Lawrence area showed no significant difference as discussed in Section 5.1.

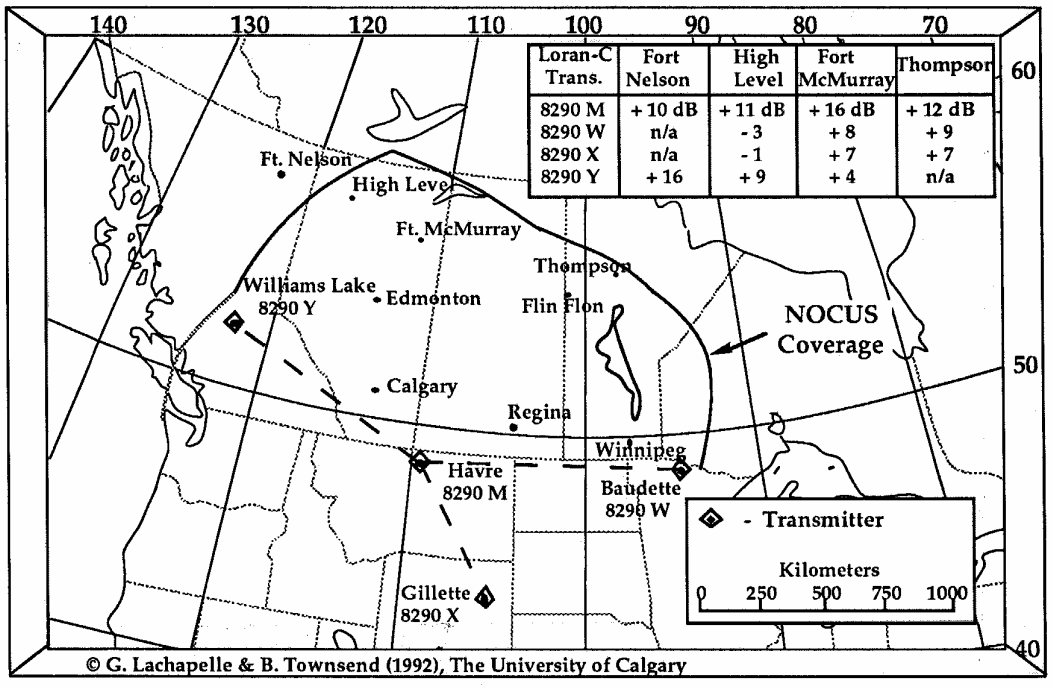

Figure 5.6: Estimated Northern Extent of NOCUS

5.3 LORAN-C Receiver Comparisons

A well-suited application of LORCAL^2 is the comparison of LORAN-C receivers. The system simultaneaously collects data from two or three receivers and this makes it possible to compare receivers of different manufacturers as well as those from the same manufacturer. The following will investigate both scenerios.

The Accufix 520 and the LocUs Pathfinder have vastly different receiver design. The Accufix 520 uses analogue technology while the Pathfinder uses digital technology. A direct comparison between the Accufix 520 and Pathfinder measurements was made between Gaspé and Carleton, Québec, during the winter of 1991. During the campaign along this 250 km road section, both units were recording data on the 5930 Chain. The differences between the DTDs measured with the Accufix 520 and the Pathfinder units are shown in Figure 5.7, 5.8 and 5.9 for 5990X, Y and Z, respectively. The mean differences are nearly zero while the rms differences are of the order of 0.12μs, which corresponds to a single measurement accuracy of $0.12\mu s/\sqrt{2}$ or 0.08μs. This is considered fully satisfactory in a vehicle dynamic environment.

The FS and SNR measured simultaneously by the Accufix 520 and the Pathfinder on the same transmitters show differences of the order of -3 to -5 dB in FS and -10 dB in SNR. In most cases, the differences are constant. The negative differences indicate that the Accufix 520 FS and SNR measurements are generally slightly lower than those made by the Pathfinder. The biases are likely due to some differences in signal processing techniques used in each receiver.

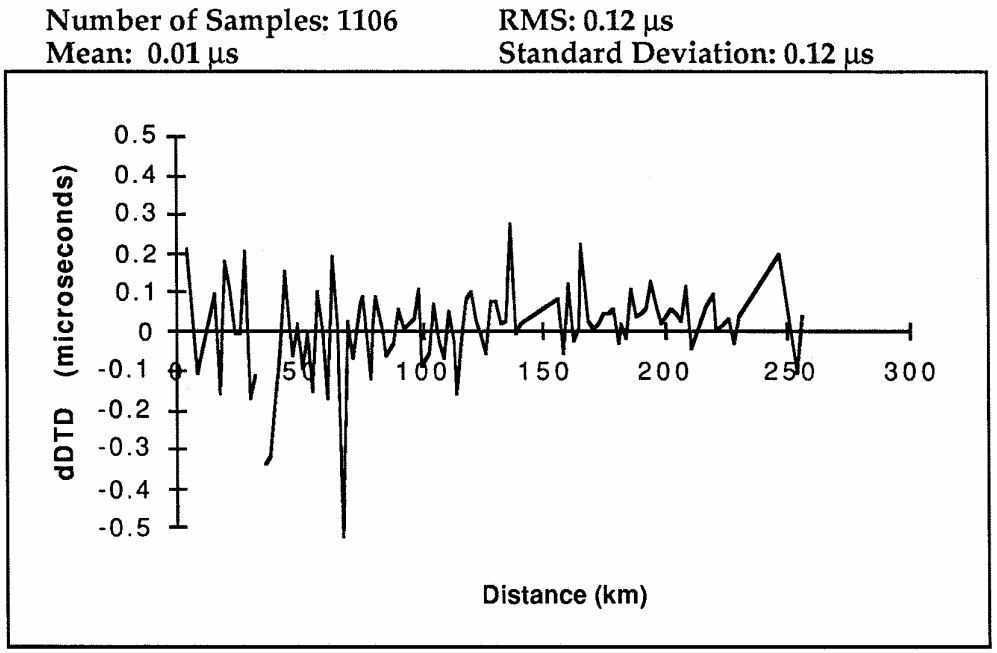

Figure 5.7: Differences Between Measured Accufix 520 and Pathfinder DTDs, Gaspé - Carleton, 5930X, Winter 1991

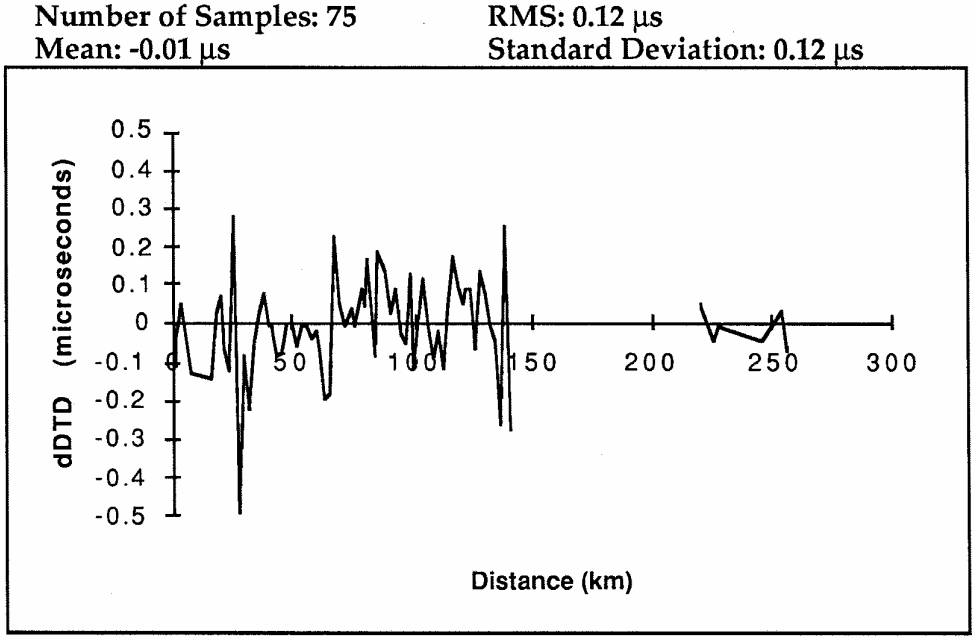

Figure 5.8: Differences Between Measured Accufix 520 and Pathfinder DTDs, Gaspé - Carleton, 5930Y, Winter 1991

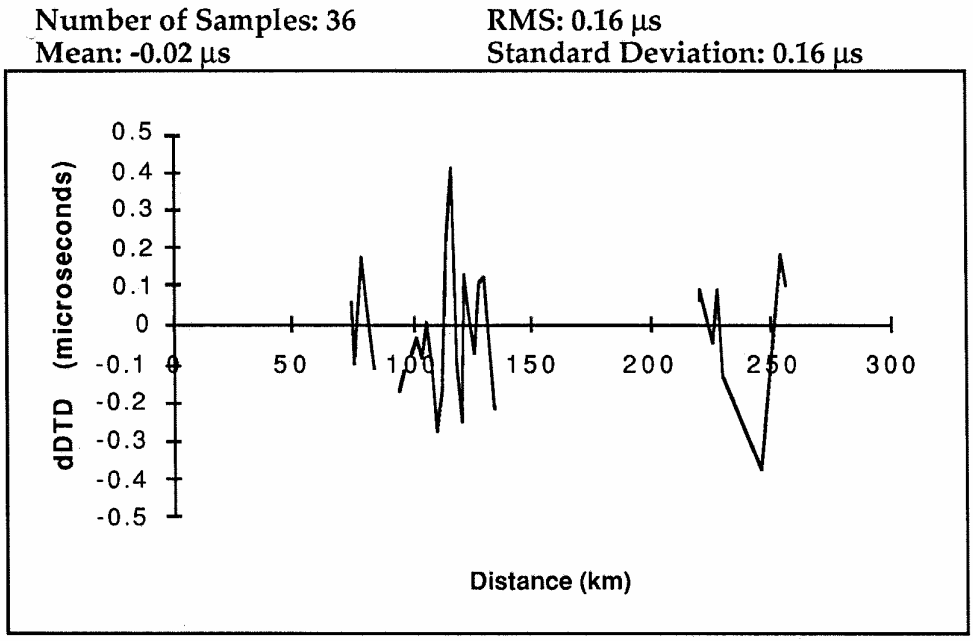

Figure 5.9: Differences Between Measured Accufix 520 and Pathfinder DTDs, Gaspé - Carleton, 5930Z, Winter 1991

In May 1992, LORCAL[2] the was used to collect data along a 230-km section of road between Osoyoos and Trail, British Columbia as shown in Figure 5.10 [Lachapelle and Townsend, 1993]. It is a mountainous road section ranging in elevation from 300 to 1100 metres. The first 50 km of road is relatively smooth compared to the next 100 km which goes through fairly rugged terrain. A three LORAN-C receiver configuration was used consisting, of two Jet 7201's and one Jet 7202.

The relative performances of the three Loran-C receivers used during the test are summarized in Tables 5.8 and 5.9 in terms of TD, SNR, FS, and ECD mean differences and rms between two receivers for each transmitter received. The smooth and rugged road sections described above were analysed separately. Table 5.8 summarizes the comparisons between the three units during the

smooth section while Table 5.9 gives the corresponding comparisons between one 7201 and one 7202 unit for the rugged section.

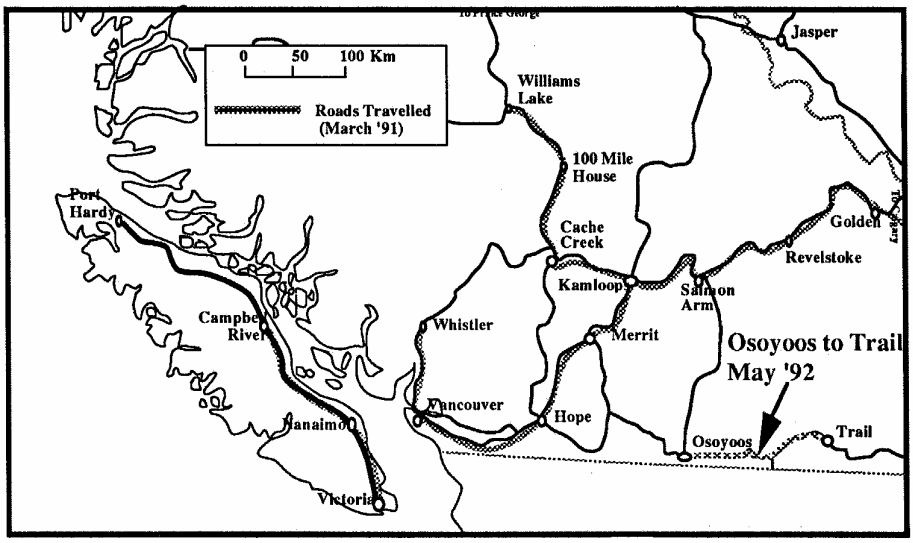

Figure 5.10: Roads Selected for GPS and Loran-C Signal Availability Analysis

The statistics presented in Table 5.8 show no significant differences in performance between the 7201 and 7202 models, apart from a constant difference in the measured field strength (FS), the 7201 Model measurements being 8.4 dB higher than the corresponding measurements with the 7202 Model. This bias is due to the longer in-house antenna used with the 7201 Model. Jet antennae (e.g., 7202 antenna) are calibrated with an accuracy of 1-2 dB. The FS measurements taken by the 7201 are, therefore, 8 dB too high. The average rms differences of 0.04 to 0.05 μs between measured TDs in Table 5.8 indicate that a TD is measured with an accuracy of 0.03μs (0.045μs/$\sqrt{2}$) or 9 m, which is better than the manufacturer's specification of 0.1μs.

The statistics presented in Table 5.9 for the rugged part of the road section are similar to those of Table 5.8 with two significant differences. The average TD

rms has increased to 0.20μs, which is due to the large variations in FS and SNR along the road. The average ECD rms has increased to 1.19μs, as compared to 0.28μs during the smooth part of the road section. The percentage of the time each transmitter signal was "good" according to the receiver tracking status is also given in Table 5.9.

Table 5.9: Intercomparison of Loran-C JET Receivers Used During Smooth Part of Road Tests

Station	TD (μs)		SNR (dB)		FS (dB)		ECD (μs)	
	mean	rms	mean	rms	mean	rms	mean	rms
1 st Model7201 - 2 nd Model 7201								
5990M			0.86	1.31	-0.04	0.74	0.09	0.31
5990Y	-0.02	0.03	0.51	1.72	0.00	0.79	0.23	0.20
5990Z	-0.07	0.05	0.29	0.59	-0.14	0.67	0.16	0.35
8290M			-0.38	0.63	-0.07	0.68	0.04	0.46
8290Y	-0.04	0.04	0.43	1.10	0.03	0.79	0.08	0.30
9940M			-0.11	0.65	-0.13	0.66	0.14	0.33
9940W	-0.01	0.03	-0.81	2.03	-0.02	0.68	0.26	0.18
Average	*-0.04*	*0.04*	*0.23*	*1.07*	*-0.04*	*0.73*	*0.12*	*0.32*
Model7201 - Model 7202								
5990M			1.10	1.64	8.54	0.69	0.17	0.19
5990Y	0.00	0.04	-0.22	2.18	8.42	0.70	0.05	0.34
5990Z	-0.01	0.07	1.66	0.97	8.40	0.72	0.13	0.45
8290M			1.02	0.90	8.22	0.65	0.22	0.44
8290Y	-0.02	0.05	-0.39	1.67	8.47	0.69	0.13	0.17
9940M			1.32	0.83	8.31	0.62	0.21	0.25
9940W	0.00	0.03	0.34	1.87	8.46	0.65	0.05	0.15
Average	*0.00*	*0.05*	*0.69*	*1.44*	*8.40*	*0.67*	*0.14*	*0.28*

Table 5.10: Intercomparison of Loran-C JET Receivers Used During Rugged Part of Road Test (Model 7201 - Model 7202)

Station	% *	TD (μs)		SNR (dB)		FS (dB)		ECD (μs)	
		mean	rms	mean	rms	mean	rms	mean	rms
5990M	75			-0.09	1.69	8.08	1.44	-0.10	0.92
5990Y	57	0.00	0.06	-0.22	1.84	8.18	0.75	0.04	0.45
5990Z	45	-0.02	0.18	0.63	1.21	8.27	1.16	0.40	1.91
8290M	63			0.02	1.46	8.05	1.04	0.44	2.11
8290Y	64	0.00	0.24	-0.57	1.97	8.12	1.18	-0.01	1.12
9940M	37			0.00	1.62	8.09	1.04	0.39	1.39
9940W	56	-0.01	0.33	-0.19	1.62	8.21	0.84	0.07	0.45
Average		*-0.01*	*0.20*	*-0.06*	*1.63*	*8.14*	*1.06*	*0.18*	*1.19*

* Percentage of the time receiver tracking status was "good".

5.4 GPS/LORAN-C For Vehiclular Navigation in Mountainous Areas

The research presented here was initiated following an extensive investigation of GPS and Loran-C signal availability along the mountainous roads of British Columbia [Lachapelle et al, 1992a]. The roads of interest are shown in Figure 5.10 of the previous section. The results of this investigation are summarized in Tables 5.11 and 5.12. The road measurements were taken in Winter 1991. Tables 5.11 and 5.12 give the GPS and Loran-C signal availability, in terms of percentage of distance, for the road sections shown in Figure 5.10. While the theoretical GPS coverage is nearly 100%, the actual coverage varies from 25% to nearly 100%. The two sections with the poorest coverage are Whistler to Vancouver and Nanaimo to Victoria. In the former case, the cause of the poor coverage is the

presence of steep mountains on the south side of the road, while in the latter case, signal masking due to a combination of steep topography and forest canopy is the main cause. Recent testing under a tree canopy with fast reacquisition receivers suggest however that GPS signal availability is strongly a function of the receiver technology used [Melgard et. al., 1994].

Table 5.11: GPS Signal Availability for Vehicular Navigation in British Columbia

Section of Road	Dist. (km)	Forward Direction				Reverse Direction			
		Theoretical GPS Coverage[1]			Actual[2] GPS Cov. % of Dist.	Theoretical GPS Coverage[1]			Actual[2] GPS Cov. % of Dist.
		Num of SV	HDOP H not fixed	HDOP H fixed		Num of SV	HDOP H not fixed	HDOP H fixed	
Golden ⇒ Revelstoke	148	4 ⇔ 5	1.3 ⇔ 3.6	1.3 ⇔ 2.0	93.7				
Revelstoke ⇒ Kamloops	212	3 ⇔ 5	2.2 ⇔ 39.3	1.2 ⇔ 15.6	87.5	4 ⇔ 5	1.5 ⇔ 5.0	1.3 ⇔ 2.1	65.5
Kamloops ⇒ Cache Cr.	79	5 ⇔ 6	1.0 ⇔ 1.6	1.0 ⇔ 1.3	>95	3 ⇔ 6	1.3 ⇔ 10.9	1.2 ⇔ 5.6	89.7
Cache Cr. ⇒ 100 Mile H.	115	5 ⇔ 6	1.5 ⇔ 2.5	1.3 ⇔ 2.0	74.5	3 ⇔ 5	1.6 ⇔ 5.9	1.1 ⇔ 2.1	46.1
100 Mile H. ⇒ Williams L.	91	4 ⇔ 5	1.9 ⇔ 24.6	1.4 ⇔ 2.1	92.6	4 ⇔ 5	1.2 ⇔ 1.5	1.1 ⇔ 1.4	50.7
Kamloops ⇒ Merrit	85	3 ⇔ 4	3.7 ⇔ 9.1	2.9 ⇔ 6.2	>95	5	1.2 ⇔ 1.6	1.2 ⇔ 1.5	81.1
Merrit ⇒ Hope	108	6	1.3 ⇔ 1.4	1.3 ⇔ 1.4	>95	4 ⇔ 5	2.2 ⇔ 18.0	1.6 ⇔ 12.4	78.4
Hope ⇒ Vancouver	174	4 ⇔ 5	1.2 ⇔ 10.6	1.2 ⇔ 17.6	90.5	3 ⇔ 6	1.3 ⇔ 6.1	1.2 ⇔ 3.3	90.9
Whistler ⇒ Vancouver	113	4 ⇔ 5	1.2 ⇔ 1.8	1.2 ⇔ 1.5	24.5				
Nanaimo ⇒ Campbell R.	154	4 ⇔ 6	1.3 ⇔ 12.8	1.2 ⇔ 5.7	53.8	4 ⇔ 5	1.6 ⇔ 65.7	1.3 ⇔ 17.7	64.4
Nanaimo ⇒ Victoria	110	3 ⇔ 5	1.8 ⇔ 1.9	1.3 ⇔ 1.5	27.5	3 ⇔ 6	1.3 ⇔ 8.3	1.2 ⇔ 6.9	64.5

1. HDOP is calculated using all satellites available above a 10 degree elevation angle.
2. Actual coverage is based on the following criteria:
   (i) HDOP < 10
   (ii) Maximum allowable data gap of 10 seconds.

LORAN-C availability is generally better than GPS but significant signal dropouts occured along certain sections. Single chain receivers were used during the measurements which were made on the West Coast Canada Chain (GRI 5990) which provides the best coverage in the area. However, two other chains are partially available in the area, namely the North Central US Chain (GRI 8290) and the West Coast US Chain (GRI 9940), as shown in Figure 5.11. The question as to whether the use of a multi-chain receiver would result in a better signal availability is, therefore, important. The two receivers used consisted of an analog (Accufix 520) and a digital unit (LocUS Pathfinder). The performance of

the LocUS unit was significantly better, presumably due to the use of a linear ensemble averaging technique [Post, 1989]. The results presented in Table 5.12 are therefore dependent on the type of receiver used. Since neither GPS nor LORAN-C in stand alone mode are likely to provide 100% coverage in the best of cases, the question becomes whether the use of GPS and LORAN-C in a combined mode would improve the coverage.

Table 5.12: Single Chain (GRI 5990) Loran-C Signal Availability for Vehicular Navigation in British Columbia

Section of Road	Dist. (km)	Receiver	Coverage (% of Dist.) [1]		Loran -C HDOP	TD's Used
			Forward Direction	Reverse Direction		
Golden ⇒ Revelstoke	148	Accufix 520	24.2	--	11.4 ⇒ 6.3	YZ
		Locus	72.3	--		YZ
Revelstoke ⇒ Kamloops	212	Accufix 520	79.2	76.3	6.3 ⇒ 2.9	YZ
		Locus	90.0	84.8		YZ
Kamloops ⇒ Cache Cr.	79	Accufix 520	>95	>95	2.7 ⇒ 2.1	YZ
		Locus	>95	>95		YZ
Cache Cr. ⇒ 100 Mile H.	115	Accufix 520	92.9	90.4	2.1 ⇒ 3.1	YZ
		Locus	>95	>95		YZ
100 Mile H. ⇒ Williams L.	91	Accufix 520	67.7	66.5	3.1 ⇒ 38.0	YZ
		Locus	>95	>95	3.1 ⇒ 1.8	XYZ
Kamloops ⇒ Merrit	85	Accufix 520	>95	>95	2.9 ⇒ 2.2	YZ
		Locus	>95	>95		YZ
Merrit ⇒ Hope	108	Accufix 520	90.0	49.5	2.2 ⇒ 1.8	YZ
		Locus	86.0	68.3		YZ
Hope ⇒ Vancouver	174	Accufix 520	68.7	69.0	1.8 ⇒ 1.4	YZ
		Locus	--	81.7		YZ
Whistler ⇒ Vancouver	113	Accufix 520	36.0	--	1.4	YZ
		Locus	80.1	--		YZ
Nanaimo ⇒ Campbell R.	154	Accufix 520	72.2	--	1.4 ⇒ 1.2	YZ
		Locus	83.8	93.8		YZ
Nanaimo ⇒ Victoria	110	Accufix 520	52.7	58.2	1.4 ⇒ 1.6	YZ
		Locus	75.9	74.6		YZ

1. Based on a maximum allowable data gap of 30 seconds and minimum SNR of -10 dB for the Accufix 520 and -15 dB for the Locus.

In order to answer some of the above questions, a field test was conducted in May 1992 along a relatively rugged 230-km road section of Southern British

Columbia, namely between Osoyoos and Trail, as shown in Figure 5.10 [Lachapelle and Townsend, 1993]. The same LORCAL^2 configuration as in Figure 4.2 was used. The topography in this area is rugged with height variations of up to a few thousands of metres. The height of the road itself varies approximately between 300 m and 1100 m. The result was variable LORAN-C and GPS coverage due terrain induced signal blockages. Before analysing the results of this field test, the integration of GPS and LORAN-C measurements will be discussed.

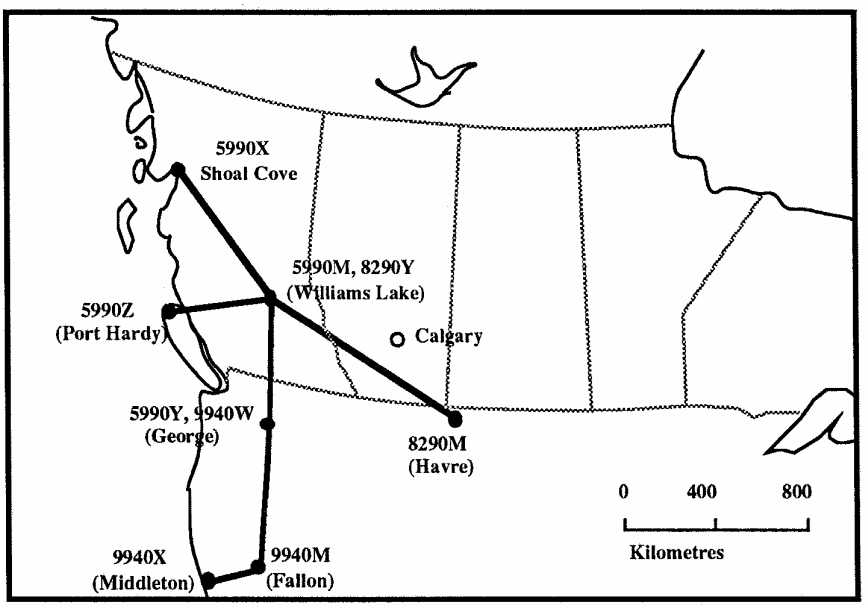

Figure 5.11: Loran-C Transmitters Available In Southern B.C.

5.4.1 Integration of LORAN-C and GPS Measurements

The JET LORAN-C receiver time delays are measured in the TOA (Time-of-Arrival) mode. These TOA measurements were converted to standard TD (Time Difference) measurements. The mathematical model for the LORAN-C TD measurements is as follows:

$$TD_1 = S_1(\phi,\lambda) - S_M(\phi,\lambda) + E_{Lor},$$

where,

TD_1 = Time difference measurement

$S_1(\phi,\lambda)$ = Distance to the Secondary transmitter

$S_M(\phi,\lambda)$ = Distance to theMaster transmitter

E_{Lor} = Unmodelled systematic biases.

There are two unknowns in this case, namely latitude (ϕ) and longitude (λ), and a minimum of two TDs are needed to calculate a position and its estimated covariance matrix. For the analysis herein, TD measurements were assumed uncorrelated and were assigned a unit weight to derive the HDOP figures shown in the next section.

In stand alone mode, GPS pseudoranges were processed using a similar technique. The mathematical model for GPS pseudorange measurements is as follows:

$$r = R(\phi,\lambda,h) - dT + E_{GPS},$$

where

r = pseudorange measurement

R = true range to satellite and is a function the latitude(ϕ), longitude(λ) and height (h) of the receiver

dT = receiver time bias

E_{GPS} = Unmodelled systematic biases.

A minimum of four satellites are required to calculate a position and covariance matrix since there are four unknowns, namely, latitude, longitude, height, and

receiver time bias. In the combined GPS/LORAN-C case, a minimum of two GPS satellites were required since two additional unknown are present when introducing GPS into the solution, the height and receiver time bias. The addition of GPS measurements does not therefore always result in a smaller HDOP than that of LORAN-C in stand alone mode. This could result in a degraded solution. In order to avoid this situation, the hydrid solution is selected only when the hydrid HDOP is better than the LORAN-C HDOP.

5.4.2 Improvement In Navigation Coverage

The results of combining GPS and LORAN-C in terms of HDOP are presented in Figures 5.12 and 5.13, for the LORAN-C multi-chain and single-chain case, respectively, and summarized in Table 5.13.

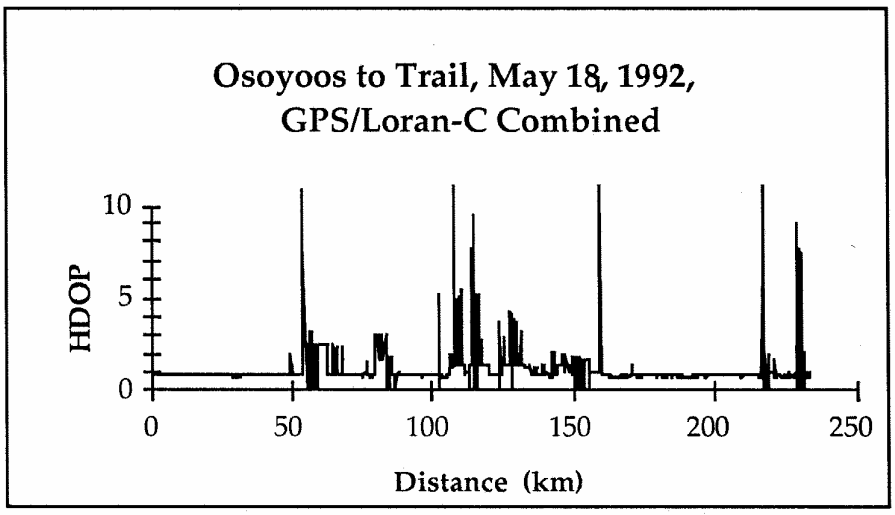

Figure 5.12: Observed Combined GPS and Multi-Chain Loran-C HDOP Between Osoyoos and Trail, B.C.

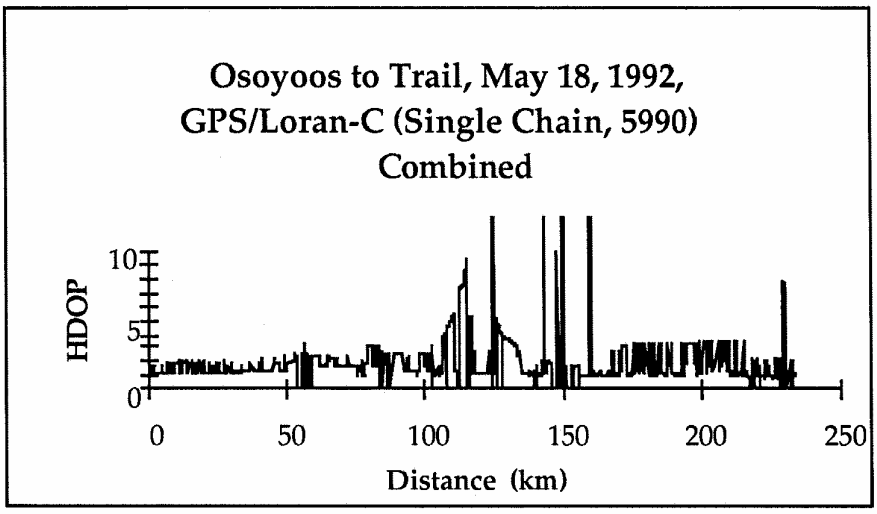

Figure 5.13: Observed Combined GPS and Single-Chain (5990) Loran-C HDOP Between Osoyoos and Trail, B.C.

The improvements over the GPS or LORAN-C in stand alone mode are significant indeed. In the multi-chain case, GPS/LORAN-C provides navigation with a HDOP ≤ 5 some 94% of the time. When a HDOP ≤ 10 is used, availability increases to 96%. The corresponding value for the single chain case is 90% (HDOP ≤ 5).

Table 5.13: Signal Availability of Loran-C, GPS and Combined GPS/Loran-C for Vehicular Navigation Between Osoyoos and Trail, British Columbia

System	Availability (% of distance)	
	HDOP ≤ 5	HDOP ≤ 10
GPS	61	65
LORAN-C (Multi Chain)	77	77
LORAN-C (Single Chain)	65	n/a
GPS/LORAN-C (Multi-Chain)	94	96
GPS/LORAN-C (Single-Chain)	90	n/a

This test, conducted along a mountain road in a rugged area of the Rocky Mountains, shows that hydrid GPS/LORAN-C improves signal availability for vehicular navigation to over 90%, as compared to approximately 60% for GPS and 75% for LORAN-C. This is a significant improvement indeed, considering the relatively small incremental cost of a LORAN-C receiver. Although the test area was selected to be representative of a typical mountainous area, the results should be extrapolated to other mountainous areas with caution, in view of the rapidly changing geometry of LORAN-C in hyperbolic mode and other factors.

5.4.3 Integrated GPS and Calibrated LORAN-C

The previous section analyses hybrid GPS/LORAN-C in terms of HDOP performance. The question still remains as to what level of positioning accuracy can be achieved. As demonstrated in Section 5.1, the LORAN-C measurement biases due to propagation delays are large, especially when over land propagation is involved. Hence, for the purposes of this analysis, it is decided to narrow the investigation to consider combining GPS with calibrated LORAN-C only.

With this purpose in mind, a data set collected on March 22, 1992, along a 60 km section of Highway 40 in the Kananaskis Valley was selected. The Kananaskis Valley is located approximately 80 km west of Calgary as shown in Figure 5.14. The topography in the area consists of 3,000 m high mountains with the valley floor ranging between 1,500 and 2,000 m in height [Townsend, 1992].

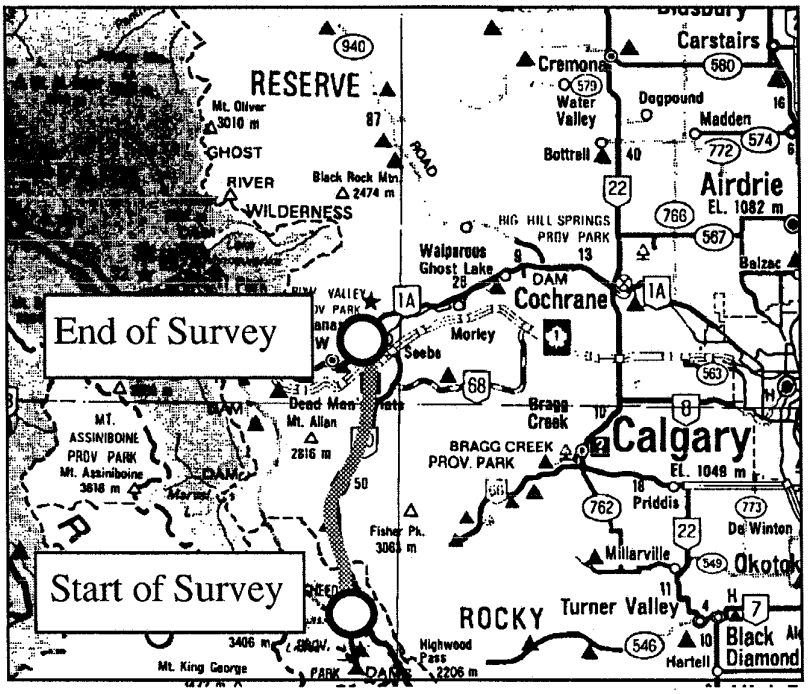

Figure 5.14: Test Road Section in the Kananaskis Valley

The Loran-C receivers were tracking transmitters from the West Coast Canada (GRI 5990) and the North Central U.S. (GRI 8290) chains. In the survey area, four TDs were usable for navigation. These are 8290W, 8290X, 8290Y and 5990Y.

The positioning accuracies of GPS and Calibrated LORAN-C are discussed for the following three cases:

(i) Calibrated LORAN-C (CLC),

(ii) Single Point GPS (SGPS), and

(iii) combined SGPS/CLC.

In each case, the positions are compared to the DGPS positions subject to a HDOP ≤ 5. The monitor was located on the roof of the Engineering Building at The University of Calgary.

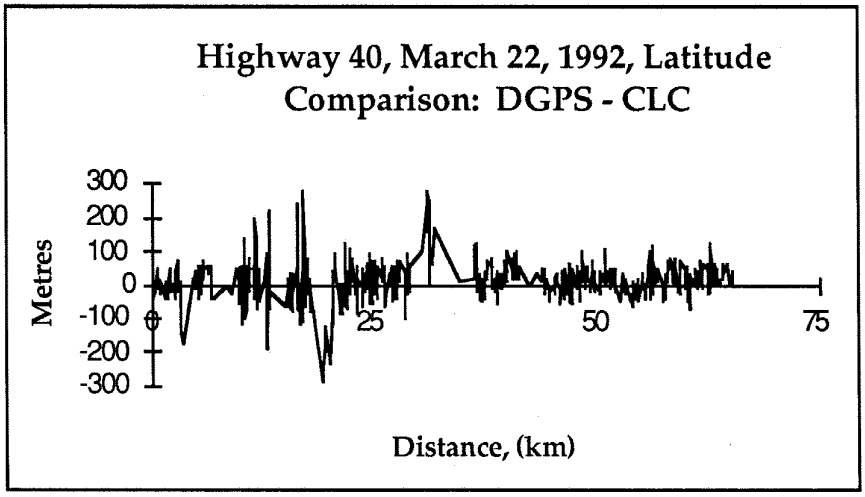

Figure 5.15 Latitude Comparison: DGPS - CLC

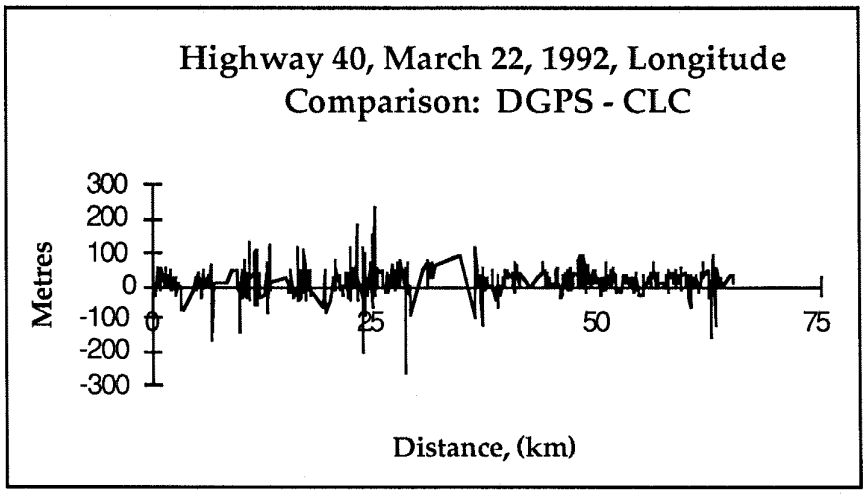

Figure 5.16: Longitude Comparison: DGPS - CLC

Figures 5.15 and 5.16 show the differences in latitude and longitude between the DGPS and the CLC positions.

The differences in latitude and, to a lesser extent, longitude, become large near the 20 km and 30 km distance marks. These large differences of up to 300 metres are correlated with problems in the LORAN-C signals from 5990Y and 8290W. In the first case, the 5990Y suffers an outage and, as a result, the LORAN-C HDOP increases to almost 5. Considering that the TD calibration is accurate to 50 - 100 m, this level of distortion is not unreasonable. In the latter case, it was found that the calibration value for 8290W is approximately 0.5 microseconds different from the measured DTD. This could be due to rapid changes in the TD calibration values caused by nearby mountains or the result of an equipment malfunction.

Figures 5.17 and 5.18 show the coordinate differences between DGPS and SGPS. As expected, the plots show differences to be systematic with a small amount of noise. This is due to the high measurement resolution of GPS and to the fact that most of the errors affecting GPS are systematic in nature (e.g., orbital, atmosphere, and SA)..

Figures 5.19 and 5.20 show the comparison of integrated SGPS/CLC to DGPS. The plots are much noisier than those in Figures 5.17 and 5.18, presumably due to the inclusion of the noisier Loran-C measurements, but the overall trend is more random; the maximum error is less than 100 m with the exception of a few points.

The mean, rms, and maximum values for the plots shown in Figures 5.15 to 5.20 are summarized in Table 5.14 for the latitude and longitude components. In all cases, the rms values are below 100 m.

Combining CLC and SGPS results in a small improvement in the longitude rms and a small degradation in the latitude rms. For reasons discussed earlier, the

Combining CLC and SGPS results in a small improvement in the longitude rms and a small degradation in the latitude rms. For reasons discussed earlier, the maximum values are quite large for CLC, as much as 280m. The maximum values for SGPS are the smallest.

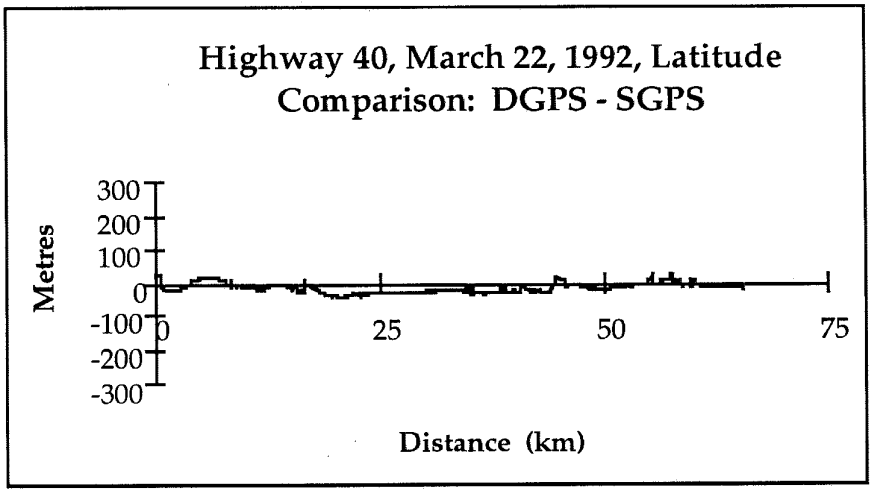

Figure 5.17: Latitude Comparison: DGPS - SGPS

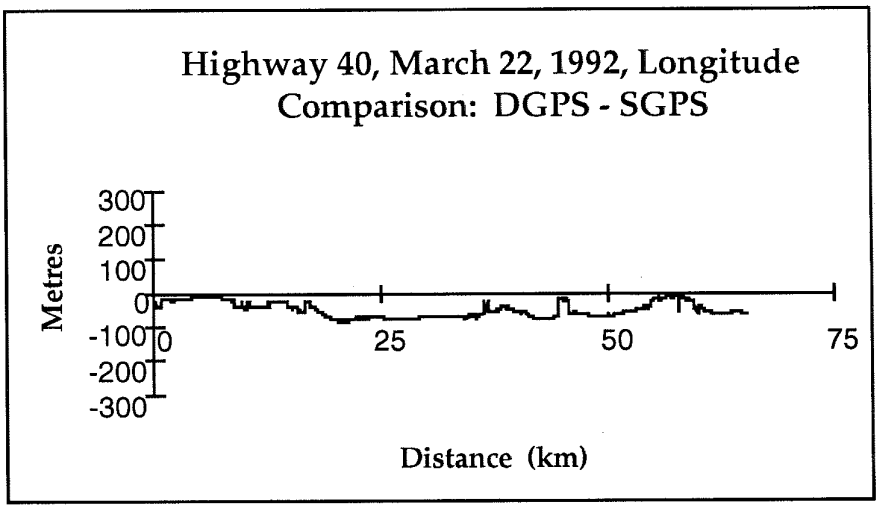

Figure 5.18: Longitude Comparison: DGPS - SGPS

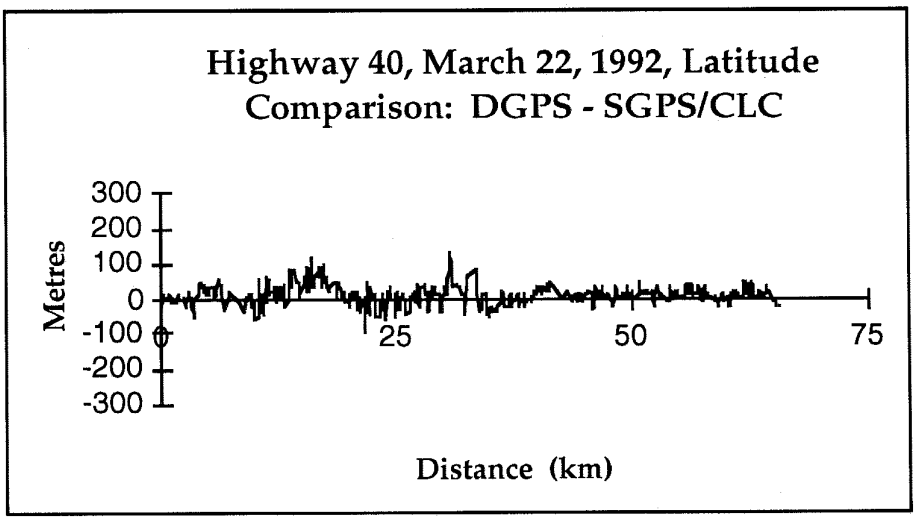

Figure 5.19: Latitude Comparison: DGPS - SGPS/CLC

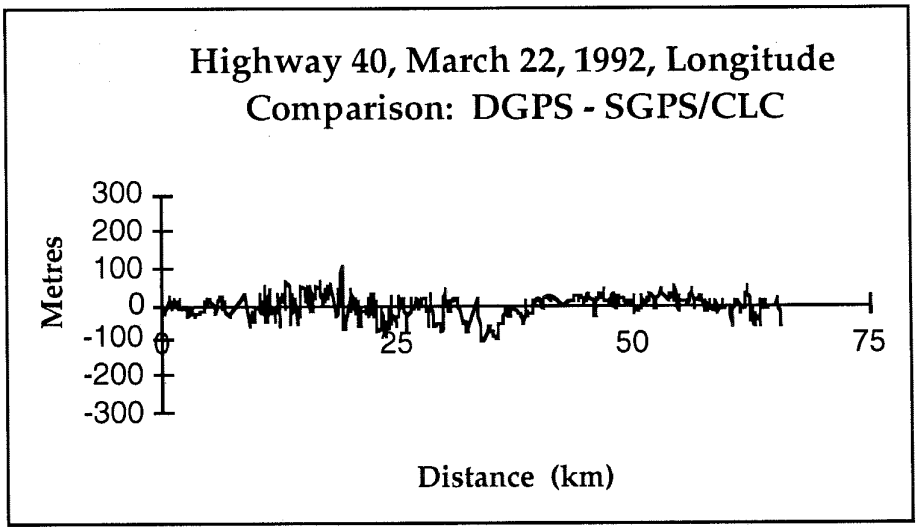

Figure 5.20: Latitude Comparison: DGPS - SGPS/CLC

Table 5.14: Comparisons Between CLC, SGPS, SGPS/CLC and DGPS

Positioning Mode	Latitude			Longitude		
	Mean (m)	RMS (m)	Max (m)	Mean (m)	RMS (m)	Max (m)
CLC	8.7	54.0	283.4	13.9	40.4	263.1
SGPS	-15.5	21.0	44.9	-51.3	55.5	86.2
SGPS/CLC	13.9	33.3	129.3	-5.8	32.6	108.7

CHAPTER 6

CONCLUSIONS AND RECOMENDATIONS

The conclusions which can be drawn from the performance of the LORCAL^2 system developed herein are as follows:

- The LORCAL^2 system has proven itself to be an effective tool for the calibration of LORAN-C signal distortions. It produced good results in both mountainous and flat terrain and a comparison of forward and reverse runs has confirmed its accuracy to be of the order of 52 m or 0.17 μs.

- The LORCAL^2 system has been shown to be an excellent tool for the analysis and comparison of both GPS and LORAN-C signals.

- The LORCAL^2 systems modular design has been shown to be valuable for various LORAN-C and GPS signal analysis tasks.

The conclusions which can be drawn from the performance of LORAN-C on land in Canada are as follows:

- The LORAN-C signals suffer large distortions over relatively short distances. Although the ground conductivity is a major factor in the propagation delays, the variation of the topography seems to cause the large fluctuations. This effect was quite pronounced in the case of the LORAN-C survey done in the Pemberton, B.C. area [Lachapelle et al, 1991].

- In the Lower St. Lawrence region, the measured Loran-C FS and SNR agreed best with predicted values when a ground conductivity of 0.001 S m^{-1} and an

atmospheric noise of 61 dB were used. This would indicate the values calculated by the CCIR [CCIR,1988a] are too optimistic.

- The GPS-derived LORAN-C distortions measured on both the East Coast Canada and Northeast U.S. Chains in the Lower St.Lawrence reach approximately 5μs. This magnitude of distortions was typical with that in other areas of the country and is largely due to radio wave propagation distortion over land.

- The residual distortions still present once the primary, secondary and additional secondary factors (using a uniform propagation path assumption) are removed, are minimized when using a conductivity value of 5 S m^{-1} on the East Coast Canada Chain and 0.001 S m^{-1} on the Northeast U.S. Chain. This is due to the influence of sea water present between most of the 5930 (East Coast Canada Chain) transmitters and the survey area which indicates a mixed path prediction model would produce even better results.

- The effect of these residual distortions on LORAN-C derived positions reaches several hundred of metres and is a function of the transmitters used and the positioning geometry.

- The seasonal and multi-year stability of LORAN-C was estimated at some 25 m, which is also well within the tolerances stipulated for the system. This would indicate the LORAN-C Area Monitors are adequate for keeping the signal stable.

- In constrast, the comparison of across chain TDs indicate the Area Monitors are introducing across chain biases in the system.

- The coverage of the NOCUS Chain reaches farther north than expected. It appears the extra coverage is due to a much lower than expected atmospheric noise.

- The use of multi-chain receivers would provide even more coverage as was shown with the northern extent of the NOCUS coverage.

The conclusions which can be drawn from the performance of Hybrid GPS/LORAN-C on land are as follows:

- Results show that integrated GPS/LORAN-C can significantly increase the navigation coverage in a mountainous area where both systems suffer degradation in accuracy and performance.

- Calibrated LORAN-C produces the postioning accuracy close to that of GPS with S.A. on. Therefore, the best results are achieved when calibrated LORAN-C measurements are used in a GPS/LORAN-C system.

The recommendations related to possible future investigations are as follows:

- LORAN-C field measurements should be made with multi-chain digital receivers to improve performance by allowing the operator to track all available LORAN-C transmitters.

- TD distortions should be calibrated individually since a LORAN-C may use various transmitter combinations for receivers in position calculations

- Since the residual effect of the TD distortions on LORAN-C derived positions is strongly a function of the transmitters actually used to obtain the fix, considerations might be given to providing position corrections based on

various transmitter combinations for receivers which do not accept individual TD corrections. Since multi-chain receivers are now commonly available to Loran-C users, these position corrections should then be extended to include multi-chain TD combinations.

REFERENCES

CCIR (1988a) **Characteristics and Applications of Atmospheric Radio Noise Data. Report No. 322-3**. International Radio Consultative Committee, International Telecommunication Union, Geneva, 1988.

CCIR (1988b) **World Atlas of Ground Conductivities**. CCIR Report No. 717-2, International Telecommunications Union, Geneva.

CHS (1983) **Notes on the Use of LORAN-C Charts**. 2nd Edition, Canadian Hydrographic Service, Department of Fisheries and Oceans, Ottawa.

FORSSELL, B. (1991) **Radionavigation Systems**. Prentice Hall International (UK) Ltd., pp.114-145.

HAMILTON, G. (1987) **Extension of Canadian Loran-C Coverage**. IRRD No. 291115, Roads and Transportation Association of Canada, Ottawa.

HUFFORD, G. A. (1952) **An Integral Equation Approach to the Problem of Wave Propagation Over an Irregular Terrain**. Quart. J. Appl. Math, 9, pp. 391..

JOHLER, J. R. (1977) **LORAN-C Propagation Error Corrections Over Inhomogeneous Irregular Ground Using the Integral Equation Technique**. CRPLI Report 77.

JOHLER, J. R., and A. R. COOK (1984) **Accurate Position Determination in the Bering Sea Using Loran-C**. Proceedings of 13th Annual Technical Symposium, The Wild Goose Association, pp. 125-154.

JOHLER, J.R., W.J. KELLAR, and L.C. WALTERS (1956) **Phase of Low Radiofrequency Ground Wave. National Bureau of Standards Circular 573**, United States Department of Commerce.

LACHAPELLE, G., D. GRAY, B. TOWNSEND, R. HARE, and K. LYNBERG (1993) **GPS and LORAN-C in Dixon Enterance: Availability, Reliability, Accuracy and Calibration**. Submitted to Geomatica, Canadian Institute of Geomatics, Ottawa, August. (CIG Ref # 252).

LACHAPELLE, G., T. SPEAKMAN, and B. TOWNSEND (1989) **Performance of Loran-C on the Canadian West Coast**. Proceedings of the 18th Annual Technical Symposium, The Wild Goose Association, pp. 135-143.

LACHAPELLE, G., and B. TOWNSEND (1990) **A Comparative Analysis of Loran-C and GPS for Land Vehicle Navigation in Canada**. Canadian Journal of Aeronautics, Canadian Aeronautics and Space Institute, Ottawa, Vol. 36, No. 1, pp. 29-32.

LACHAPELLE, G., and B. TOWNSEND (1991) **En-Route Coverage Validation and Calibration of Loran-C with GPS. GPS World**, Volume 2, No. 3, pp. 36-41.

LACHAPELLE, G., and B. TOWNSEND (1993) **GPS/LORAN-C: An Effective System Mix for Vehicular Navigation in Mountainous Areas**. Navigation, Vol. 40, No. 1,The Institute of Navigation, VA, pp. 19-34.

LACHAPELLE, G., B. TOWNSEND, and D. HALAYKO (1992a) **Analysis of GPS and Loran-C Performance for Land Vehicle Navigation in the Canadian Rockies**. I.E.E.E. Aerospace and Electronic Systems Magazine, New York, Vol. 7, No. 5, pp. 24-28.

LACHAPELLE, G., B. TOWNSEND, and D. HALAYKO (1992b) **Extent of the LORAN-C North Central U.S. (NOCUS) Chain in Western Canada.** Presented at the ION National Technical Meeting, San Diego, CA, January 27-29.

LACHAPELLE, G., B. TOWNSEND, and D. HAINS (1993) **Analysis and Calibration of Loran-C Signals in the Lower St. Lawrence Using GPS.** International Hydrographic Review, Monaco, Vol. LXX, No. 2, pp. 7-27.

LACHAPELLE, G., B. TOWNSEND, and B.B. MYERS (1992c) **Analysis of Loran-C Performance in the Pemberton Area, B.C.** Canadian Journal of Aeronautics, Canadian Aeronautics and Space Institute, Ottawa, Vol. 38, No. 2, pp. 52-61.

MELGARD, T., G. LACHAPELLE, and H. GEHUE (1994) **GPS Signal Availability In An Urban Area - Receiver Performance Analysis.** Proceedings of IEEE PLANS '94, Las Vegas, 11-15 April, (in press).

MOUSSA, R. (1990) **Hybridation GPS - Loran C**: Aspect Géométrique. Navigation, Institut Français de Navigation, Paris, pp. 361-370.

POST, K.E. (1989) **Real-Time Linear Ensemble Averaging Loran Receiver Architecture**. Proceedings of the 45th Annual Meeting, The Institute of Navigation, Washington, D.C., pp. 67-75.

ROHAN, P. (1991) **Introduction to Electromagnetic Wave Propagation.** Artech House, Boston.

RTAC (1987) **Extension of Canadian Loran-C Coverage.** Technical Report, Roads and Transportation Assocation of Canada, Ottawa.

SAMADDAR, S.N. (1979) **The Theory of Loran-C Ground Wave Propagation - A Review.** Navigation, Vol. 26, No. 3, pp. 173-187, Washington, D.C.

SAMADDAR, S.N. (1980) **Weather Effect on Loran-C Propagation.** Navigation: Journal of The Institute of Navigation, Vol. 27, No. 1, pp. 39-53.

SEGAL, B., and R.E. BARRINGTON (1977) **The Radio Climatology of Canada - Tropospheric Refractivity Atlas for Canada.** CRC Report No. 1315-E, Department of Communications, Ottawa.

TOWNSEND, B. (1992) **Integration of GPS and Calibrated Loran-C for Land Vehicle Navigation in Mountainous Areas.** Proceedings of ION GPS-92, Fifth International Technical Meeting of the Satellite Division of the Institute of Navigation, Albuquerque, New Mexico.

TOWNSEND, B., G. LACHAPELLE, and D. HAINS (1992a) **Loran-C Signal Analysis in the Lower St. Lawrence Using a Mobile GPS System.** Lighthouse, Canadian Hydrographic Association, 45, Ottawa. pp. 39-44.

US DoT (1992) **FAA Loran Coverage Diagrams.** Prepared by National Field Office for LORAN Data Services, DTS-502, Volpe National Transportation Systems Center, Cambridge, MA.

VIEHWEG, C.S., R.D. CROWELL, A. AVERIN, and R. H. FRAZIER (1988) **Differential Loran-C System (DLCS) Project - A Status Report.** Proceedings of the 17th Annual Technical Symposium, Wild Goose Association, Bedford, MA., pp. 187-202.

WATSON, G. N. (1918) **The Tranmission of Electric Waves Around the Earth.** Proc. Roy. Soc. A95, 83.

WELLS, D. E., N. BECK, D. DELIKARAOGLOU, A. KLUESBERG, E. J. KRAKIWSKY, G. LACHAPELLE, R. B. LANGLEY, M. NAKIBOGLOU, K. P. SCHWARZ, J. M. TRANQUILLA AND P. VANICEK (1987) **Guide to GPS Positioning**, University of New Brunswick Graphic Services, Fredricton.